Electronic Supplementary Information for:

Dramatic Enhancement in pH Sensitivity and Signal Intensity through Ligand Modification of a Dicobalt PARACEST Probe

Agnes E. Thorarinsdottir and T. David Harris*

Department of Chemistry, Northwestern University, Evanston, IL, 60208, USA

Email: *dharris@northwestern.edu*

Chemical Communications

Table of Contents

Experimental Section

General Considerations. Unless otherwise specified, the manipulations described below were carried out at ambient atmosphere and temperature. Air- and water-free manipulations were performed under a dinitrogen atmosphere in a Vacuum Atmospheres Nexus II glovebox or using standard Schlenk line techniques. Glassware was oven-dried at 150 °C for at least 4 h and allowed to cool in an evacuated antechamber prior to use in the glovebox. Acetonitrile (MeCN), diethyl ether (Et_2O), *N*,*N*-diisopropylethylamine (DIPEA), and methanol (MeOH) were dried using a commercial solvent purification system from Pure Process Technology and stored over 3 or 4 Å molecular sieves prior to use. H_2O was obtained from a purification system from EMD Millipore. Deuterated solvents were purchased from Cambridge Isotope Laboratories. The synthesis of *N*,*N*′-[(2-hydroxy-5-nitro-1,3-phenylene)bis-(methylene)]bis[*N*-(carboxymethyl)glycineamide] (HL) was carried out as reported previously.[1] All other reagents and solvents were purchased from commercial vendors and used without further purification.

Synthesis of (2-amino-1-hydroxyethane-1,1-diyl)bis(phosphonic acid) (H_4L'). This compound was synthesized following a modified literature procedure.[2] Under an atmosphere of dinitrogen, a colorless 1.0 M catecholborane solution in tetrahydrofuran (THF) (10.8 g, 11.3 mmol) was added to solid glycine (0.274 g, 3.65 mmol) at 25 °C. The resulting white suspension was stirred at 25 °C for 3 h to give a colorless solution. To this stirring solution, tris(trimethylsilyl) phosphite (4.47 g, 15.0 mmol) was slowly added and the resulting colorless solution was stirred at 25 °C for additional 22 h. Then MeOH (5 mL) was added to give a spongy white suspension and stirring was continued for 1 h at 25 °C. The volatiles were removed under reduced pressure to give a white residue which was triturated with MeOH (20 mL) to afford a white solid. The solid was stirred in THF (15 mL) for 1.5 h to wash, collected by vacuum filtration, and washed with Et_2O (2 × 5 mL). Recrystallization from H_2O and drying under reduced pressure afforded the title compound as a white powder (0.172 g, 21%). ^{1}H NMR (500 MHz, D_2O, 25 °C): δ 3.48 (t, $^3J_{HP}$ = 11.9 Hz, 2H). ^{13}C{^{1}H} NMR (126 MHz, D_2O, 25 °C): δ 70.70 (t, $^1J_{CP}$ = 137.3 Hz), 42.75 (s). ^{31}P{^{1}H} NMR (202 MHz, D_2O, 25 °C): δ 14.95 (s).

Synthesis of $Na[LCo_2L']\cdot 3.8NaNO_3\cdot 5.9H_2O$ (3). A pink solution of $Co(NO_3)_2\cdot 6H_2O$ (58.7 mg, 0.202 mmol) in H_2O (2 mL) was added dropwise to a stirring yellow suspension of HL (42.9 mg, 0.101 mmol) in H_2O (3 mL) to give an orange solution. To this solution, a colorless solution of H_4L' (22.3 mg, 0.101 mmol) in H_2O (2 mL) was added dropwise. The pH of this solution was adjusted to 7.5 by addition of a dilute sodium hydroxide solution in H_2O. The resulting dark orange solution was stirred at 25 °C for 2.5 h. The solvent was removed under reduced pressure and the obtained orange solid was washed by stirring in MeCN (15 mL) for 40 min. The resulting orange powder was collected by vacuum filtration, washed with Et_2O (15 mL), and dried under reduced pressure for 24 h to give **3** (101 mg, 83%). Anal. Calcd. for $C_{18}H_{38.8}Co_2N_{11.8}Na_{4.8}O_{31.3}P_2$: C, 17.84; H, 3.23; N, 13.64%. Found: C, 17.87; H, 3.15; N, 13.57%. ICP-OES: Co:P = 1.01:1.00. UV-visible absorption spectrum (37 μM; 50 mM 4-(2-hydroxyethyl)-1-piperazineethanesulfonic acid (HEPES) buffered to pH 6.98, 25 °C): 371 nm (ε = 12400 M^{-1} cm^{-1}). UV-visible diffuse reflectance spectrum: 370 nm. ESI-MS (*m*/*z*): Calcd. for $C_{18}H_{27}Co_2N_8O_{14}P_2$ ($[LCo_2L']^-$): 758.98, found: 759.06; calcd. for $C_{18}H_{29}Co_2N_8O_{14}P_2$ ($[LCo_2L'+2H]^+$): 760.99, found: 760.99. FT-IR (ATR, cm^{-1}): 3280 (broad, m); 3172 (broad, m); 1667 (s); 1595 (m); 1497 (w); 1471 (w); 1353 (s); 1313 (s); 1095 (s); 1031 (m); 970 (m); 876 (w); 834 (w); 752 (w); 659 (m); 597 (m); 556 (m). Slow diffusion of MeCN vapor into a concentrated solution of **3** in H_2O (pH ca. 6) afforded light orange plate-shaped crystals. However, despite repeated attempts, crystals suitable for single-crystal X-ray diffraction analysis

could not be obtained for **3**. Note that changing the pH of the H_2O solution of **3**, and exchanging the Na^+ ions for NMe_4^+ ions also only gave weekly diffracting crystals of the dicobalt complex.

Preparation of Fetal Bovine Serum (FBS) and Gelatin Gel Samples. Samples of **3** in FBS were prepared by dissolving solid samples of **3** in commercially available FBS (Fisher Scientific, catalog no. MT35010CV) and adjusting the pH to the desired values by addition of minimal amounts of dilute aqueous hydrochloric acid and sodium hydroxide solutions. To prepare 17% (w/v) gelatin gel samples of **3**, 8 mM solutions (0.60 mL) of **3** in 50 mM HEPES buffers containing 100 mM NaCl were added to NMR tubes containing gelatin powder (0.10 g) from bovine skin (Sigma Aldrich, catalog no. G9391). The resulting suspensions were heated by hot air and thoroughly shaken to form homogeneous, orange mixtures. The mixtures were slowly cooled to ambient temperature and further cooled to 4 °C and stored at that temperature for 2 h to form the gels. The pH values of the gelatin gel samples were recorded immediately following ^{1}H NMR and CEST data acquisition by submerging a pH electrode in the gels. The recorded pH values of the gels were 0.15–0.24 pH units lower than those of the HEPES buffer solutions used to prepare the samples. Note that an analogous decrease in pH was observed for gelatin gels prepared using HEPES buffer solutions without **3**. Further note that the concentration of **3** (as determined by inductively-coupled plasma optical emission spectroscopy) did not change significantly upon formation of the gels, thus 17% (w/v) gelatin gels containing 8 mM of **3** were used for experiments.

NMR Spectroscopy. ^{1}H and ^{31}P{^{1}H} NMR spectra for ligand H_4L' were collected at 25 °C at 500 and 202 MHz frequencies, respectively, on an Agilent DD2 500 MHz (11.7 T) spectrometer. The ^{13}C{^{1}H} NMR spectrum for H_4L' was collected at 25 °C at 126 MHz frequency using a Bruker Avance III 500 MHz (11.7 T) system equipped with a DCH CryoProbe. ^{1}H NMR spectra for **3** in D_2O and for aqueous solution samples containing 50 mM HEPES and 100 mM NaCl buffered to various pH values were collected on an Agilent DD2 500 MHz (11.7 T) spectrometer at 37 °C. ^{1}H NMR spectra for **3** in solutions containing 50 mM HEPES and 100 mM NaCl buffered to pH 7.4 with/without the presence of various physiological phosphate ions, in FBS, and in 17% (w/v) gelatin gels were recorded at 37 °C on a Bruker Neo 600 MHz (14.1 T) system equipped with a QCI-F CryoProbe. For samples in HEPES buffers, FBS, and gelatin, spectra were acquired using an inner capillary containing D_2O to lock the samples. All chemical shift values (δ) are reported in ppm and coupling constants (J) are reported in Hertz (Hz). The ^{1}H NMR spectrum for H_4L' is referenced to the residual proton signal from the D_2O solvent at 4.79 ppm. The ^{31}P{^{1}H} NMR spectrum for H_4L' is referenced to an external standard of 85% (v/v) phosphoric acid solution in D_2O (δ = 0 ppm). The ^{13}C{^{1}H} NMR spectrum for H_4L' in D_2O was recorded with 5% (v/v) MeOH added as an internal reference (δ = 49.50 ppm). For measurements of **3** in D_2O or other aqueous media, the chemical shift of the solvent signal in the ^{1}H NMR spectra was set to 0 ppm to simplify comparison between ^{1}H NMR spectra and the corresponding CEST spectra (Z spectra). The MestReNova 10.0 NMR data processing software was used to analyze and process all recorded NMR spectra. T_1 relaxation times of H_2O were measured on a Varian Inova 500 MHz (11.7 T) instrument after detuning the probe to account for radiation damping and obtained by fitting the H_2O signal intensities from experiments with an array of relaxation times implemented in the program *vnmr*.

Determination of pK_a by ^{1}H NMR Analysis. The pH-dependent ^{1}H NMR chemical shifts of the two methylene resonances from the ancillary bisphosphonate ligand $(H_nL')^{(4-n)-}$ (n = 1, 2) were used to estimate the pK_a value for **3**. The change in ^{1}H NMR chemical shift for each methylene resonance as a

function of pH was fit to a Boltzmann sigmoidal function[3] to model a single ionization event according to the following equation:

$$\delta = A_2 + (A_1 - A_2)/(1 + \exp((\mathrm{pH} - \mathrm{p}K_a)/dx)) \quad (1)$$

In this equation, δ is the obtained chemical shift, A_2 is the theoretical chemical shift of the fully deprotonated species, A_1 is the theoretical chemical shift of the fully protonated species, pK_a is the inflection point of the graph, and dx is a parameter describing the steepness of the curve.

CEST Experiments. All CEST experiments were carried out at 37 °C on a Varian Inova 500 MHz (11.7 T) spectrometer. For these experiments, 5–9 mM samples of **3** in aqueous buffer solutions containing 50 mM HEPES and 100 mM NaCl or in FBS or in 17% (w/v) gelatin gels at desired pH values (measured with a pH electrode before and/or after ^{1}H NMR and CEST data collection) were measured. Z-spectra (CEST spectra) were obtained according to the following protocol: ^{1}H NMR spectra were acquired from −50 to 130 ppm with a step increase of 1 ppm using a presaturation pulse applied for 2 s at a power level (B_1) of 22 μT. An inner capillary containing D_2O was placed within the NMR sample tubes to lock the samples. The normalized integrations of the H_2O signal from the obtained spectra were plotted against frequency offset to generate a Z-spectrum, where direct saturation of the H_2O signal was set to 0 ppm. CEST intensities are reported as %CEST = [(1 − M_z/M_0) × 100%] (M_z and M_0 are the magnetization on-resonance and off-resonance values, respectively). The ratios of the CEST signal intensities at 48 and 67 ppm ($CEST_{48\ ppm}/CEST_{67\ ppm}$) were used to construct the pH calibration curves.

Exchange rate constants (k_{ex}) were calculated following a previously reported method,[4] where the x-intercept ($-1/k_{ex}^2$) was obtained from a plot of $M_z/(M_0 - M_z)$ against $1/\omega_1^2$ (ω_1 in rad s^{-1}). ^{1}H NMR spectra were acquired at various presaturation power levels ranging from 14 to 22 μT applied for 6 s at 37 °C. The B_1 values were calculated based on the calibrated 90° pulse on a linear amplifier. To correct for baseline variations between the Z-spectra obtained using different presaturation powers, a linear baseline was applied for two CEST regimes. The data points at 75 and 60 ppm, and at 60 and 30 ppm were employed for the CEST peaks at 67 and 48 ppm, respectively.

Solution Magnetic Measurements. The solution magnetic moment of compound **3** was determined using the Evans method,[5] by collecting variable-pH ^{1}H NMR spectra at 37 °C (310 K) on a Bruker Avance III HD 500 MHz (11.7 T) spectrometer. In a typical experiment, the compound (2–3 mM) was dissolved in a mixture of 2% (v/v) *tert*-butanol in an aqueous solution containing 50 mM HEPES and 100 mM NaCl buffered to a specific pH value. The resulting solution was placed in an NMR tube containing a sealed capillary with the same solvent mixture but without the to-be-characterized paramagnetic compound as a reference solution. Diamagnetic corrections were carried out based on the empirical formula of the compound (as determined by elemental analysis) using Pascal's constants.[6] The paramagnetic molar susceptibility χ_M^{para} (cm^3 mol^{-1}) was calculated using the following equation:[5]

$$\chi_M^{para} = (3\Delta\nu M_w)/(4\pi\nu_0 m) - \chi_M^{dia} \quad (2)$$

In this equation, $\Delta\nu$ is the frequency difference (Hz) between the *tert*-butyl resonance of *tert*-butanol in the sample and reference solutions, M_w is the molecular mass of the paramagnetic compound (g mol^{-1}), ν_0 is the operating frequency of the NMR spectrometer (Hz), m is the concentration of the paramagnetic compound (g cm^{-3}), and χ_M^{dia} is the diamagnetic contribution to the molar susceptibility (cm^3 mol^{-1}).

UV-visible Absorption Spectroscopy. Solution and solid-state UV-visible spectra were collected at ambient temperature in the 200–800 nm range on an Agilent Cary 5000 UV-visible-NIR spectrometer

equipped with an integrating sphere for diffuse reflectance measurements. Solution spectra were collected for 34–49 μM samples of **3** in aqueous buffer solutions containing 50 mM HEPES and 100 mM NaCl at three different pH values, covering the range used for CEST experiments. A diffuse reflectance spectrum was collected on a solid sample of **3**. A sample for the measurement was prepared by mixing a solid sample of **3** with $BaSO_4$ powder for a 2-fold dilution to give a smooth, homogeneous powder. The data were treated with a background correction of $BaSO_4$ and the spectrum is reported as normalized Kubelka-Munk transformation F(R) of the raw diffuse reflectance spectrum, where F(R) was normalized with the strongest absorbance set to F(R) = 1.

Electrochemical Measurements. Cyclic voltammetry measurements were carried out at ambient temperature in an MBraun LABstar glovebox, operated under a humid dinitrogen atmosphere. A standard one-compartment cell and a CH Instruments 760c potentiostat were employed for the measurements. The cell consisted of a glassy carbon electrode as a working electrode, a platinum wire as a counter electrode, and a saturated calomel electrode (SCE) as a reference electrode. A sample of **3** was measured in an aqueous solution with 100 mM NaCl and 50 mM HEPES buffered to pH 7.4. All potentials were converted and referenced to the normal hydrogen electrode (NHE), using a literature conversion factor.[7]

Other Physical Measurements. Electrode-based pH measurements were carried out using a Thermo Scientific Orion 9110DJWP double junction pH electrode connected to a VWR sympHony B10P pH meter. The pH meter was calibrated using standardized pH buffer solutions at 4.01, 7.00, and 10.00 purchased from LaMotte Company. Elemental analysis of **3** was conducted by Midwest Microlab Inc. An infrared spectrum of a solid sample of **3** was recorded on a Bruker Alpha FTIR spectrometer equipped with an attenuated total reflectance accessory. These data are provided in Figure S1. Electrospray ionization mass spectrometry **(**ESI-MS) measurements were performed on a Bruker AmaZon SL quadrupole ion trap instrument. All measurements were carried out in MeOH carrier solvent using positive and/or negative ionization mode. Inductively-coupled plasma optical emission spectroscopy (ICP-OES) was performed on a Thermo iCAP 7600 dual view ICP-OES instrument equipped with a CETAC ASX520 240-position autosampler. Samples were dissolved in a 3% (v/v) nitric acid solution in H_2O and the emissions for Co and P were compared to standard solutions.

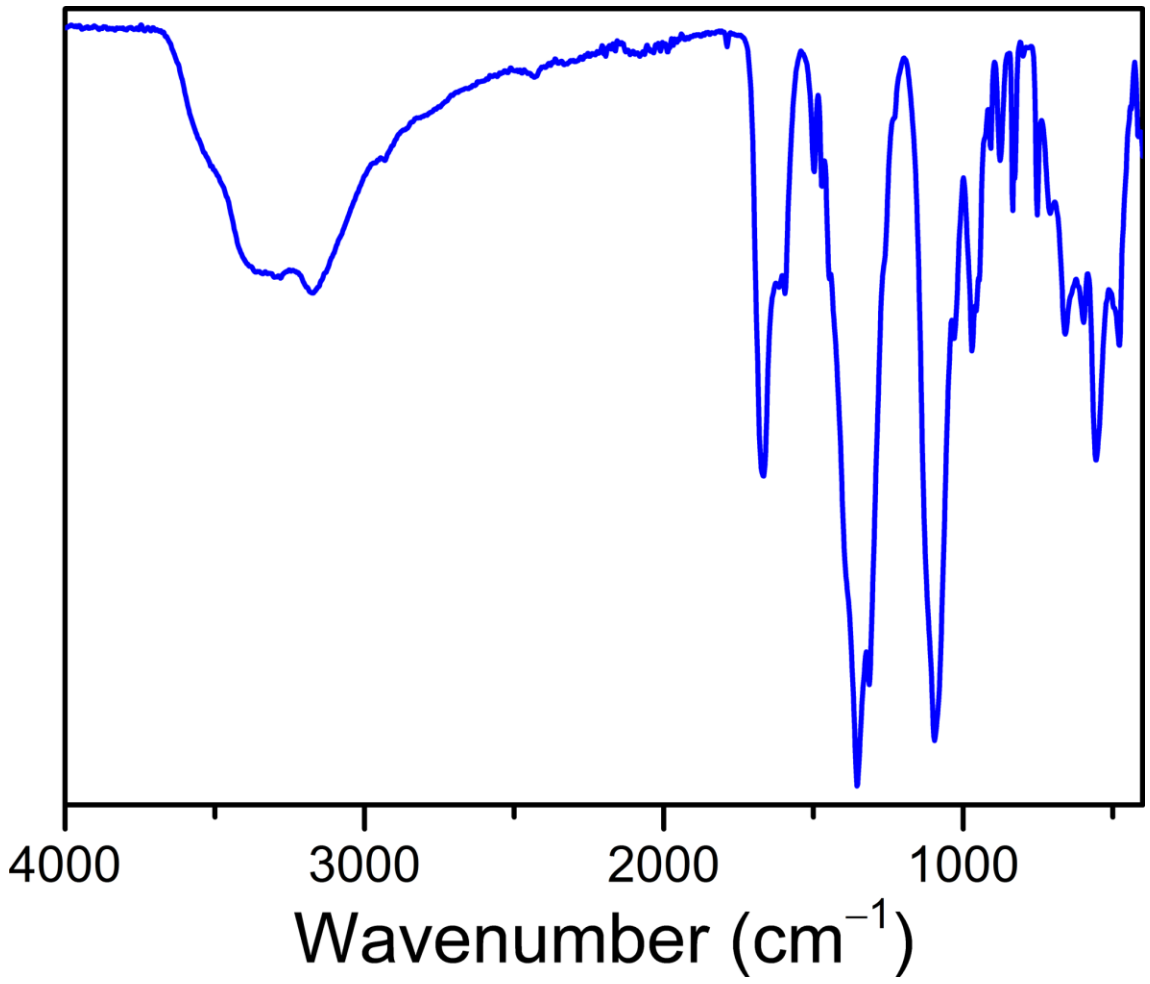

Figure S1 | FT-IR spectrum of a solid sample of **3** at ambient temperature.

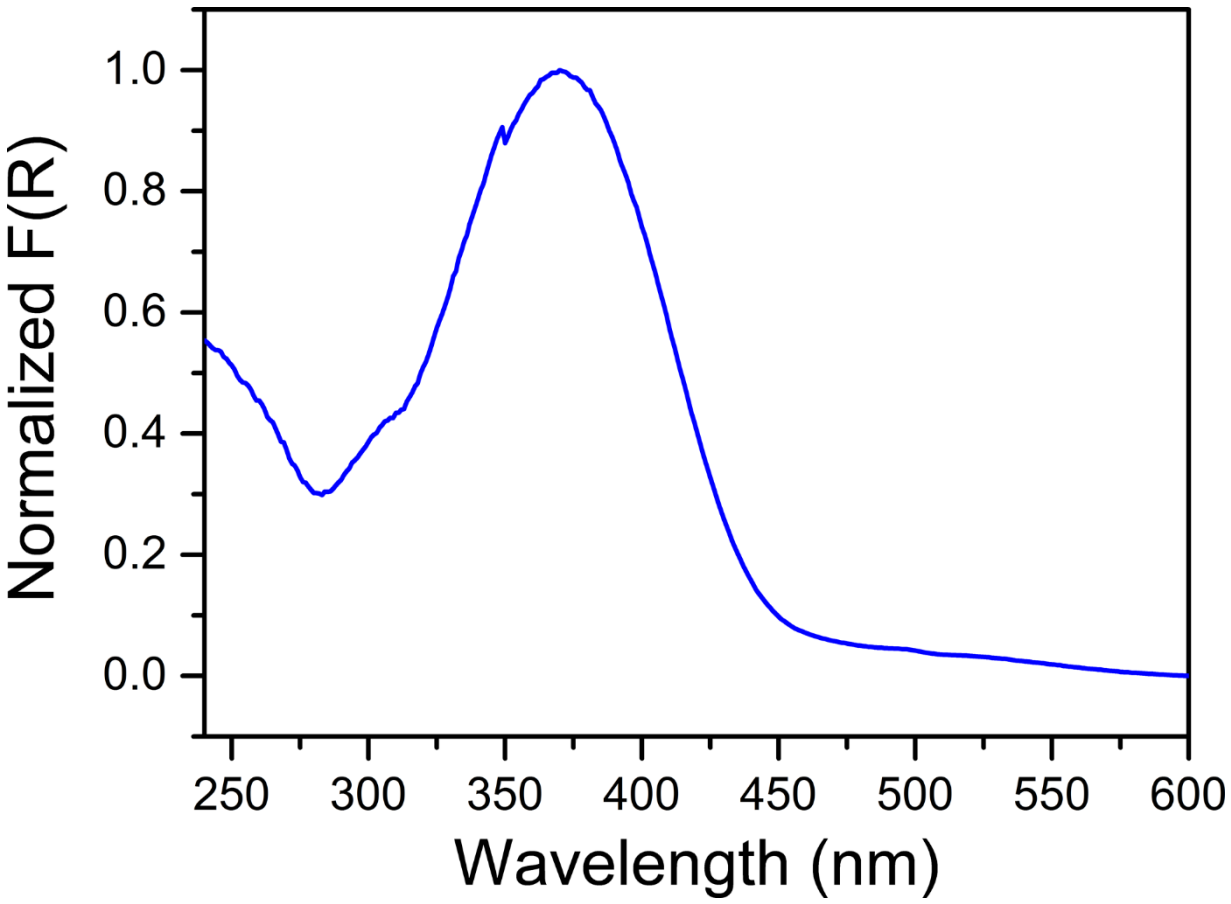

Figure S2 | Diffuse reflectance UV-visible spectrum of a solid sample of **3** diluted with $BaSO_4$ powder at ambient temperature. The spectrum is plotted as normalized Kubelka-Munk transformation F(R).

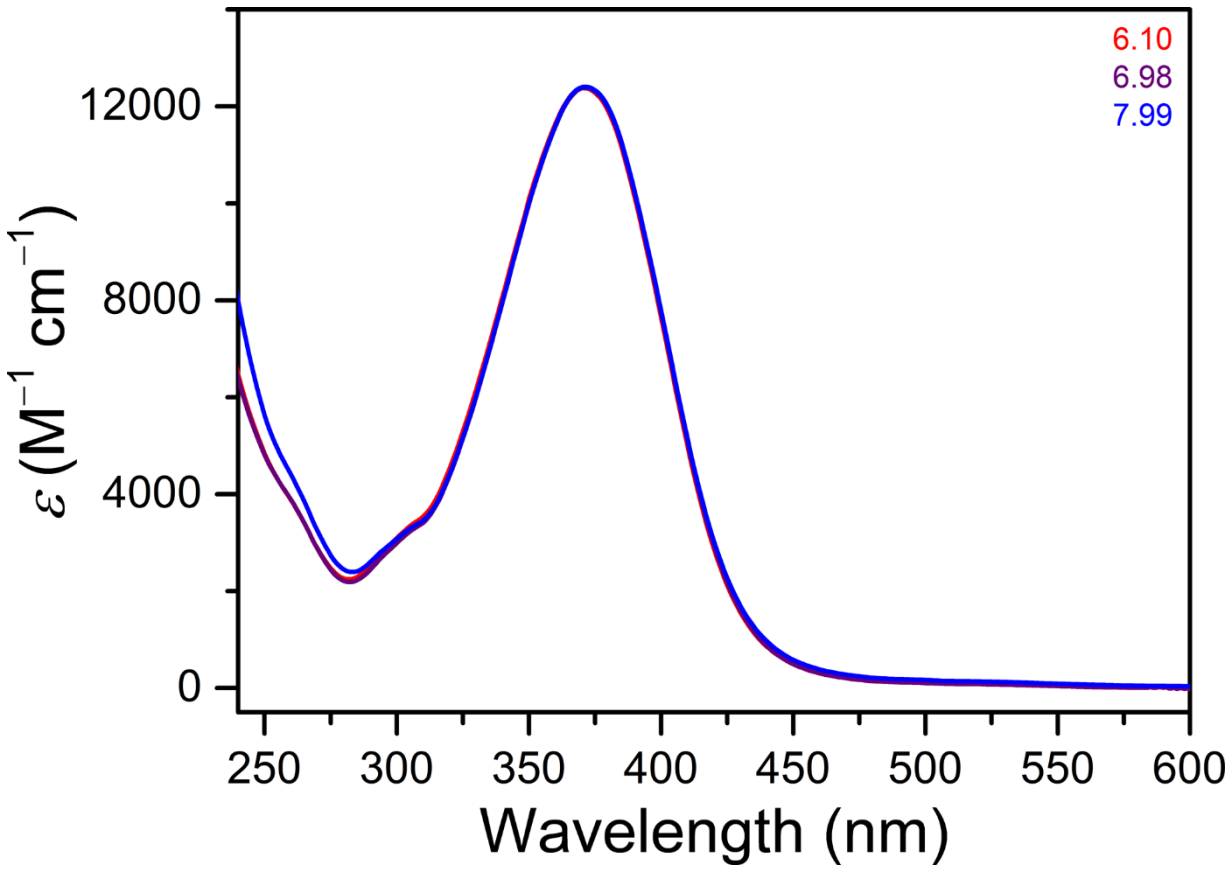

Figure S3 | Variable-pH UV-visible absorption spectra of 34–49 μM of **3** in aqueous solutions containing 50 mM HEPES and 100 mM NaCl at ambient temperature. Spectra were measured in the pH range used for CEST experiments, from pH 6.10 to 7.99. Colored numbers in the legend denote the pH of the solutions measured with a pH electrode and the corresponding color for each sample. Note that the molar absorptivity (ε) is plotted against wavelength.

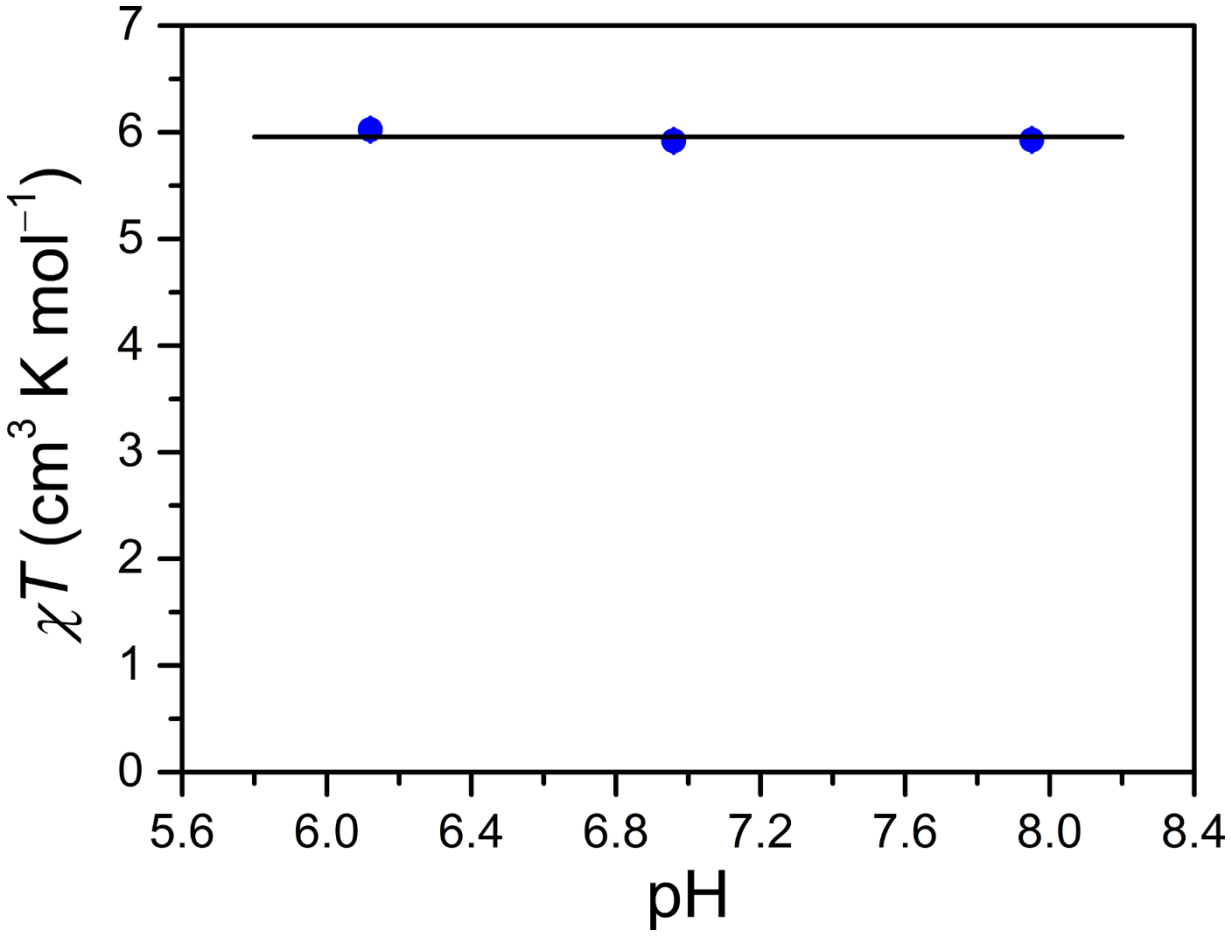

Figure S4 | Variable-pH dc magnetic susceptibility data for **3** in aqueous solutions containing 50 mM HEPES and 100 mM NaCl, collected at 37 °C and 11.7 T using the Evans method[5] (see Equation 2 in the Experimental Section). Blue circles represent experimental data and the solid black line denotes the average value of $\chi_M T$ = 5.96(6) cm^3 K mol^{-1} (see Table S1).

Table S1 | Summary of the average solution magnetic susceptibility data for **3**, collected at 37 °C and 11.7 T using the Evans method[5] (see Equation 2 in the Experimental Section) for aqueous solutions with 50 mM HEPES and 100 mM NaCl buffered to various pH values (see Figure S4).

Average values	**3**
$\chi_M T$ ($cm^3\,K\,mol^{-1}$)	5.96(6)
$\chi_M T$ per Co^{II} ($cm^3\,K\,mol^{-1}$)	2.98(3)
μ_{eff} per Co^{II} (μ_B)[a]	4.88(7)
g per Co^{II} [b]	2.52(2)

[a] The relationship between μ_{eff} and $\chi_M T$ is as follows: $\mu_{eff} = (8\chi_M T)^{1/2}\mu_B$.

[b] The relationship between $\chi_M T$ and g is as follows: $\chi_M T = (g^2 S(S+1))/8$. Note that here $S = {}^3/_2$.

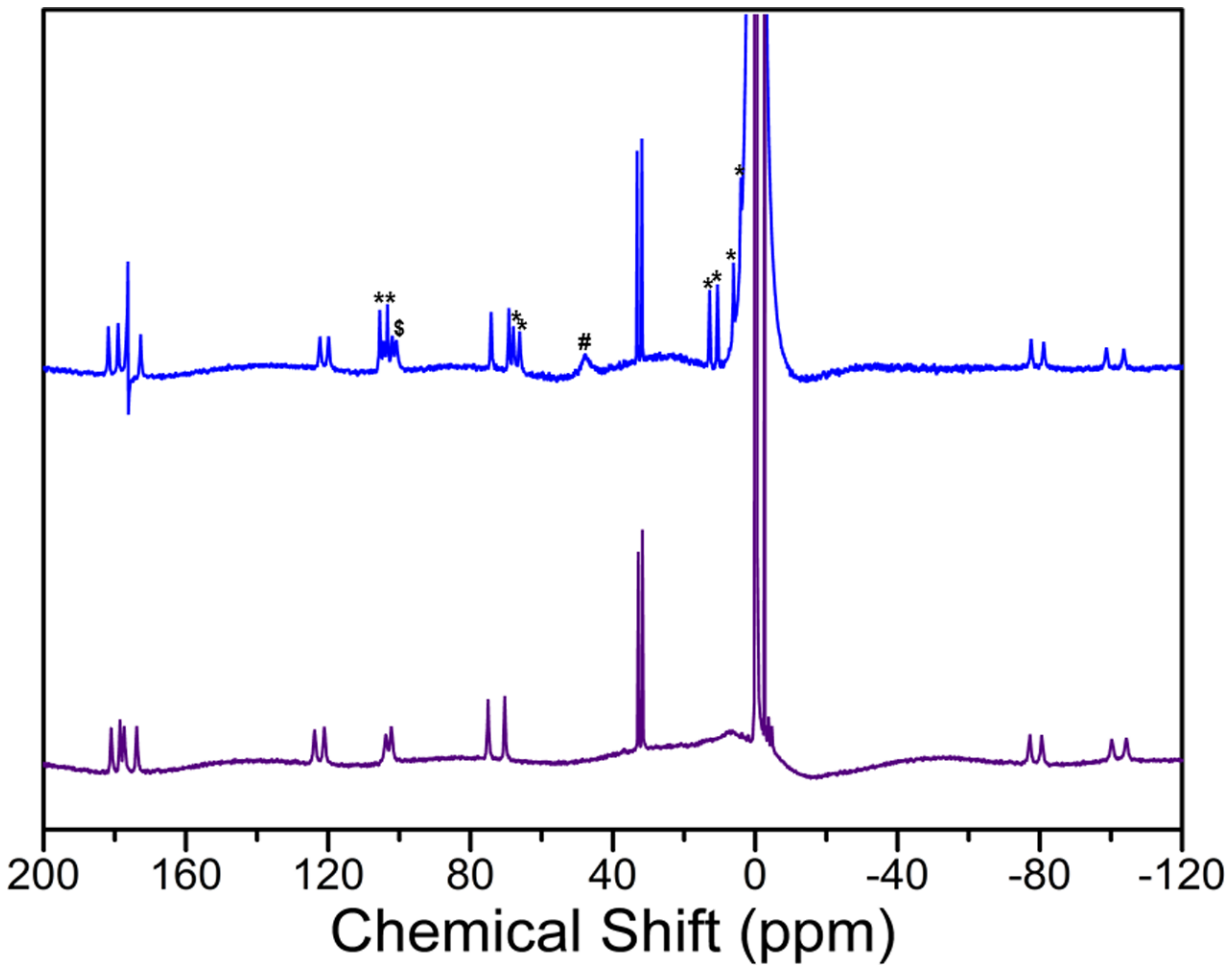

Figure S5 | Stacked ^{1}H NMR spectra of **3** in an aqueous solution containing 50 mM HEPES and 100 mM NaCl buffered to pH 7.02 (blue) and in neutral D_2O (purple), collected at 37 °C and 11.7 T. The labelled peaks correspond to exchangeable ligand protons that are not present in the spectrum recorded in D_2O. In particular, the asterisks (*) denote peaks corresponding to amide protons from the tetra(carboxamide) ligand, and the dollar sign ($) and hashtag sign (#) correspond to hydroxyl and amine protons, respectively, from the ancillary bisphosphonate ligand. The sharp feature at 176 ppm in the spectrum recorded in buffer is an instrument-derived artifact.

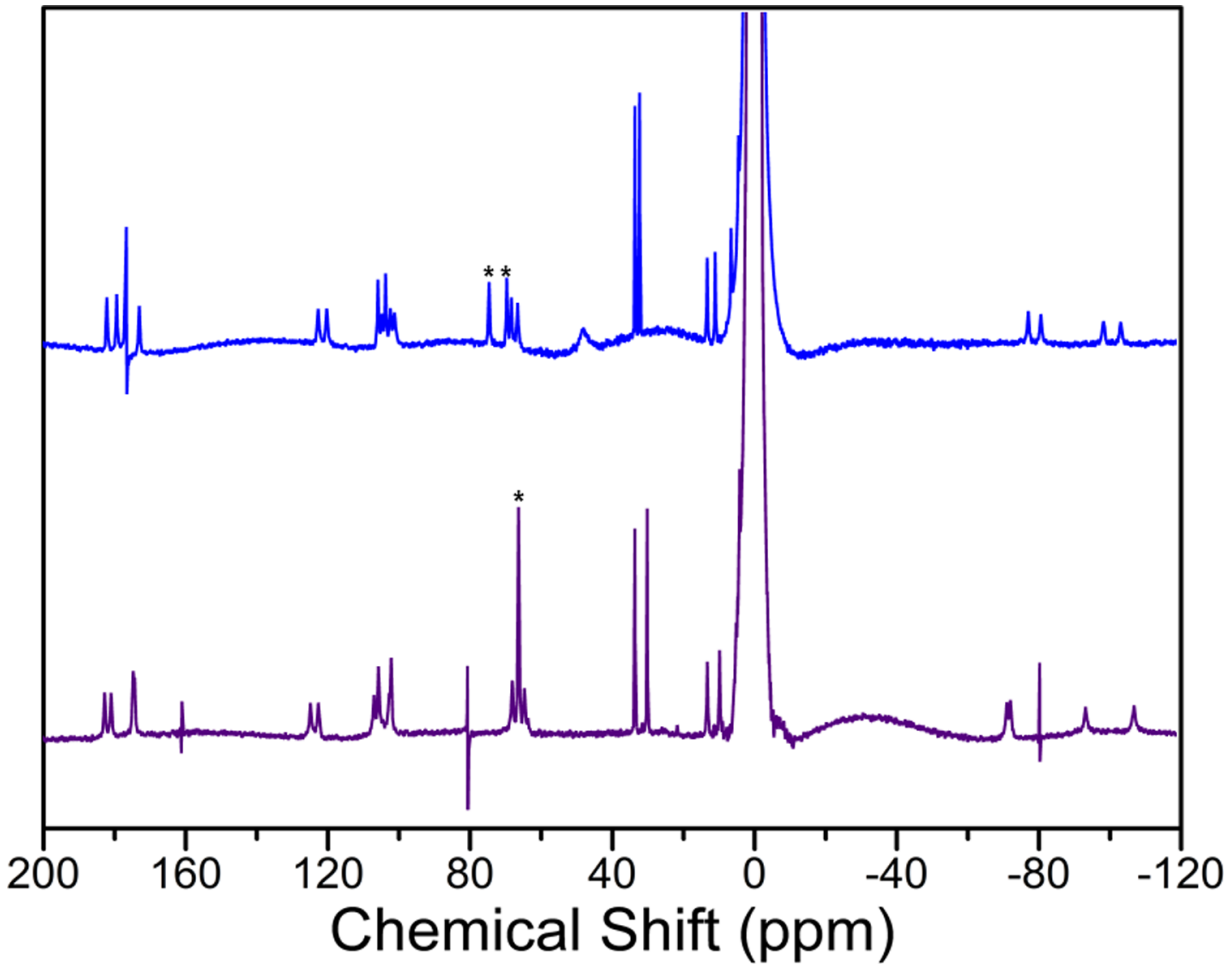

Figure S6 | Stacked ^{1}H NMR spectra of **3** (blue) and **1** (purple) in aqueous solutions containing 50 mM HEPES and 100 mM NaCl buffered to pH 7.02 and 7.06, respectively, collected at 37 °C and 11.7 T. The asterisks denote non-exchangeable proton resonances from the ancillary bisphosphonate ligands. The sharp feature at 176 ppm in the spectrum of **3** and the features at 161, 80, and −80 ppm in the spectrum of **1** are instrument-derived artifacts.

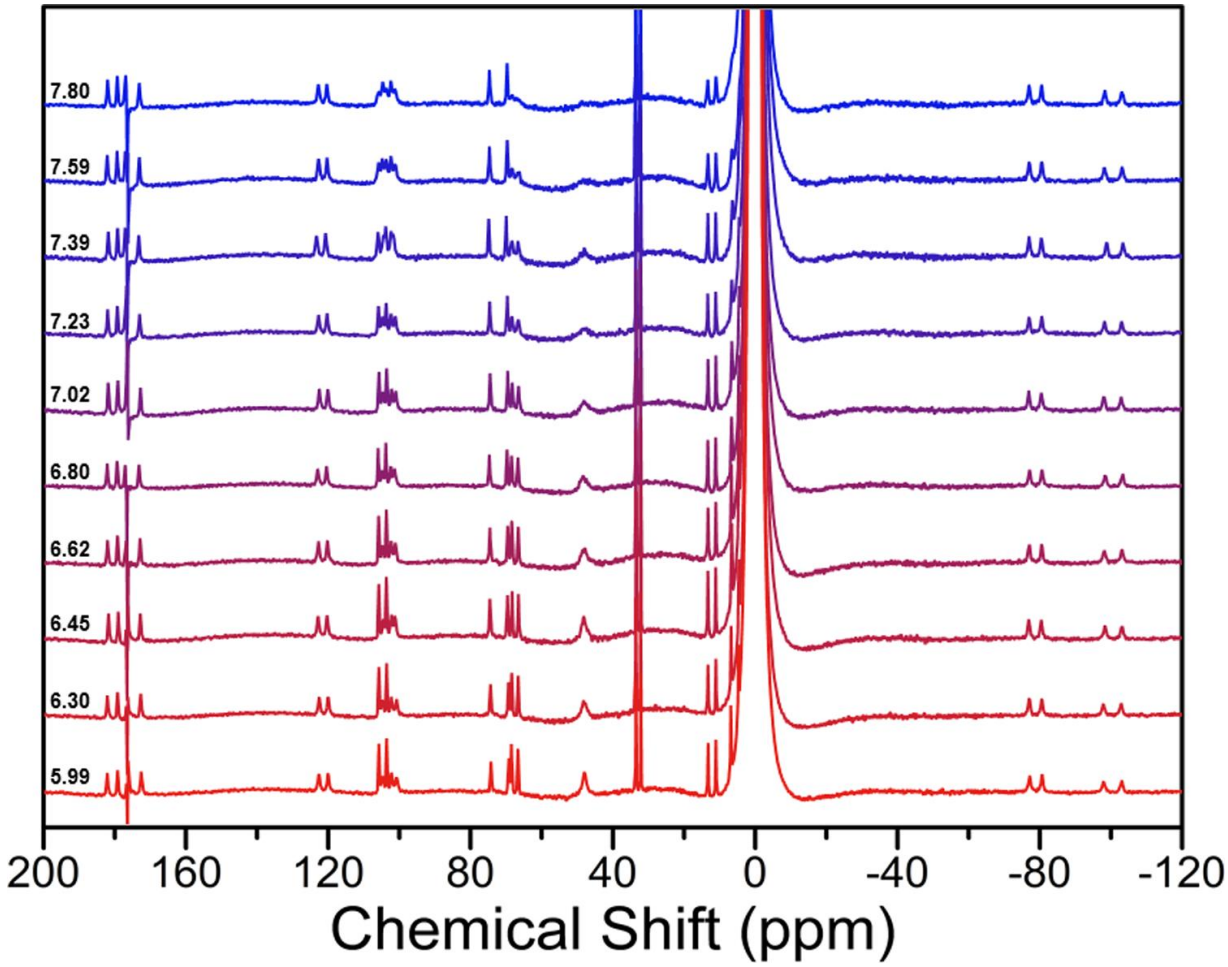

Figure S7 | Variable-pH ^{1}H NMR spectra of 10 mM of **3** in aqueous solutions containing 50 mM HEPES and 100 mM NaCl buffered to various pH values, collected at 37 °C and 11.7 T. Black numbers on the left denote the pH of the NMR sample solutions measured with a pH electrode. The sharp feature at 176 ppm is an instrument-derived artifact.

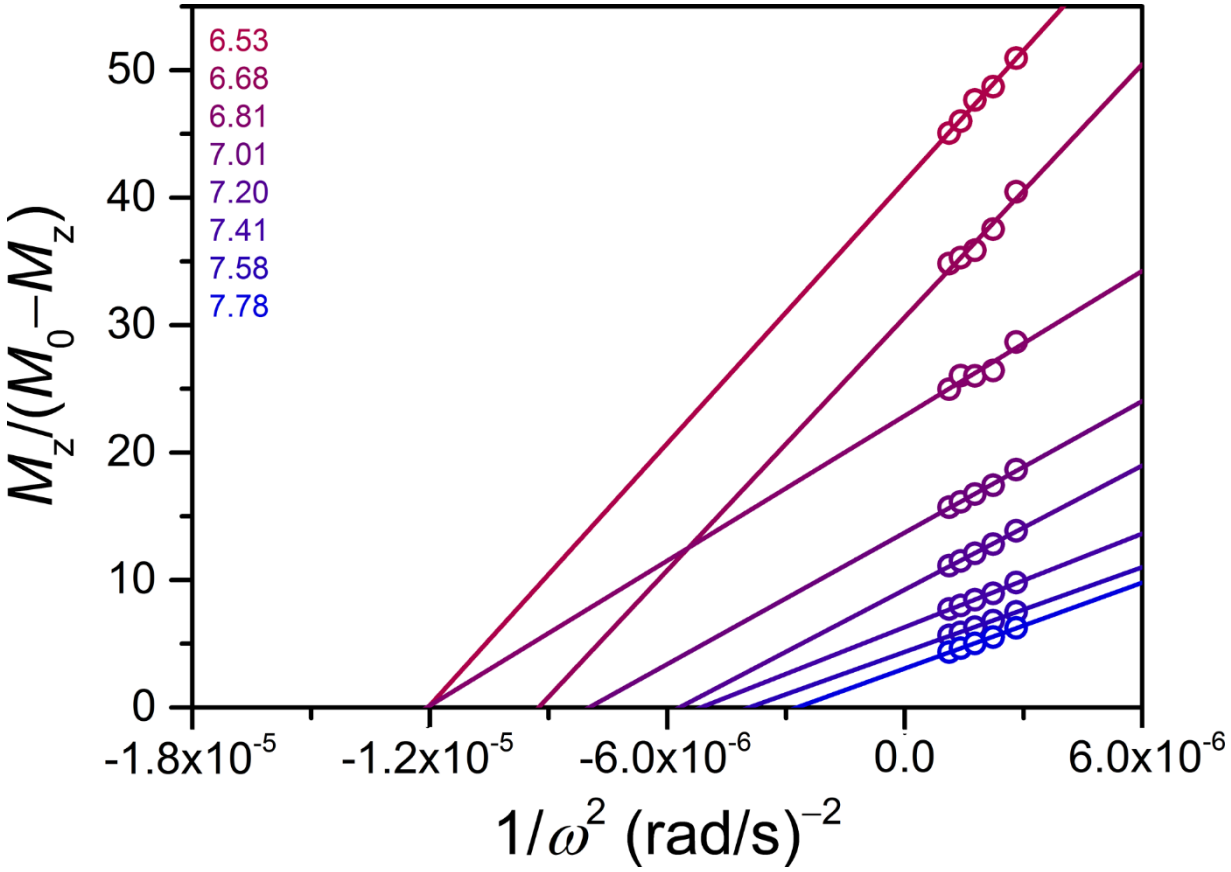

Figure S8 | Omega plots of the CEST effect from application of 6 s presaturation at 67 ppm using B_1 = 14–22 μT for 9 mM of **3** in aqueous solutions containing 50 mM HEPES and 100 mM NaCl buffered to pH 6.53–7.78 (reddish purple to blue), collected at 37 °C and 11.7 T. Colored numbers in the legend denote the pH of the solutions measured with a pH electrode and the corresponding color for each sample. Circles represent experimental data and lines represent linear fits to the data. Note that for pH values below 6.53, the amide CEST effect did not change when the presaturation power was varied from 14 to 22 μT, which indicates very slow proton exchange. Therefore, the exchange rate constant could not be estimated for those pH values using the Omega plot method.

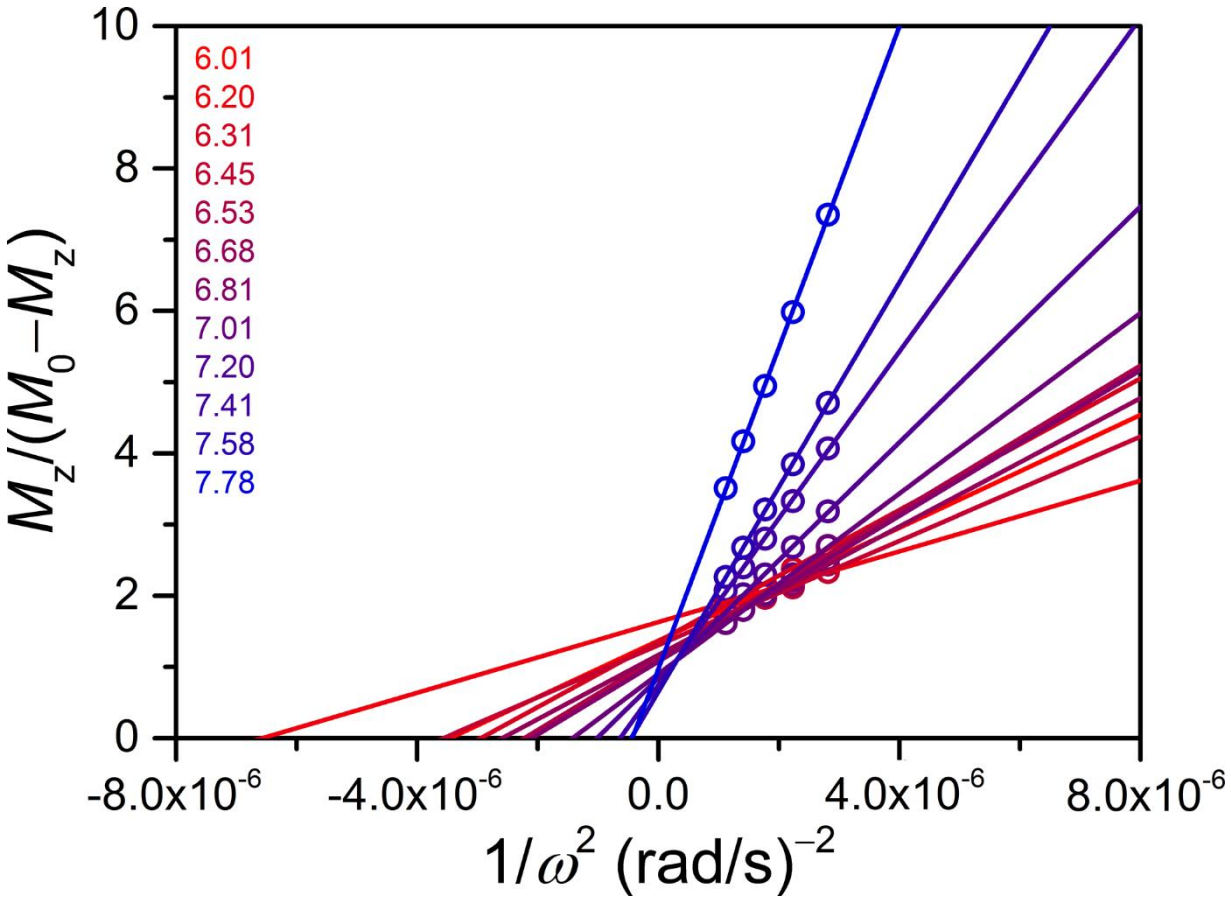

Figure S9 | Omega plots of the CEST effect from application of 6 s presaturation at 48 ppm using B_1 = 14–22 μT for 9 mM of **3** in aqueous solutions containing 50 mM HEPES and 100 mM NaCl buffered to pH 6.01–7.78 (red to blue), collected at 37 °C and 11.7 T. Colored numbers in the legend denote the pH of the solutions measured with a pH electrode and the corresponding color for each sample. Circles represent experimental data and lines represent linear fits to the data.

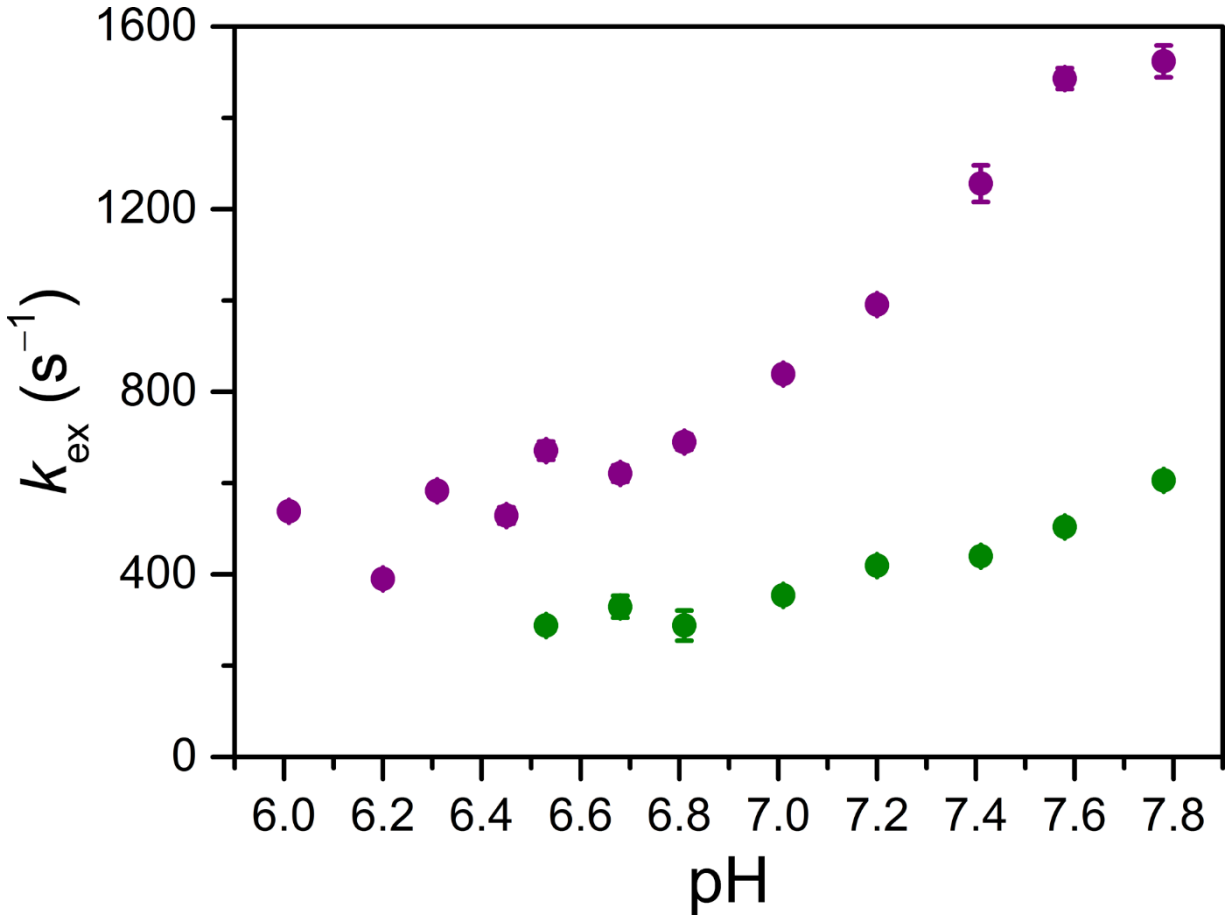

Figure S10 | pH dependences of the proton exchange rate constants (k_{ex}) for the CEST effects at 48 ppm (purple) and 67 ppm (green) for 9 mM of **3** in aqueous solutions containing 50 mM HEPES and 100 mM NaCl at 37 °C and 11.7 T, obtained from Omega plots. Circles represent experimental data and error bars represent standard deviations of the linear fits to the Omega plot data (see Figures S8 and S9).

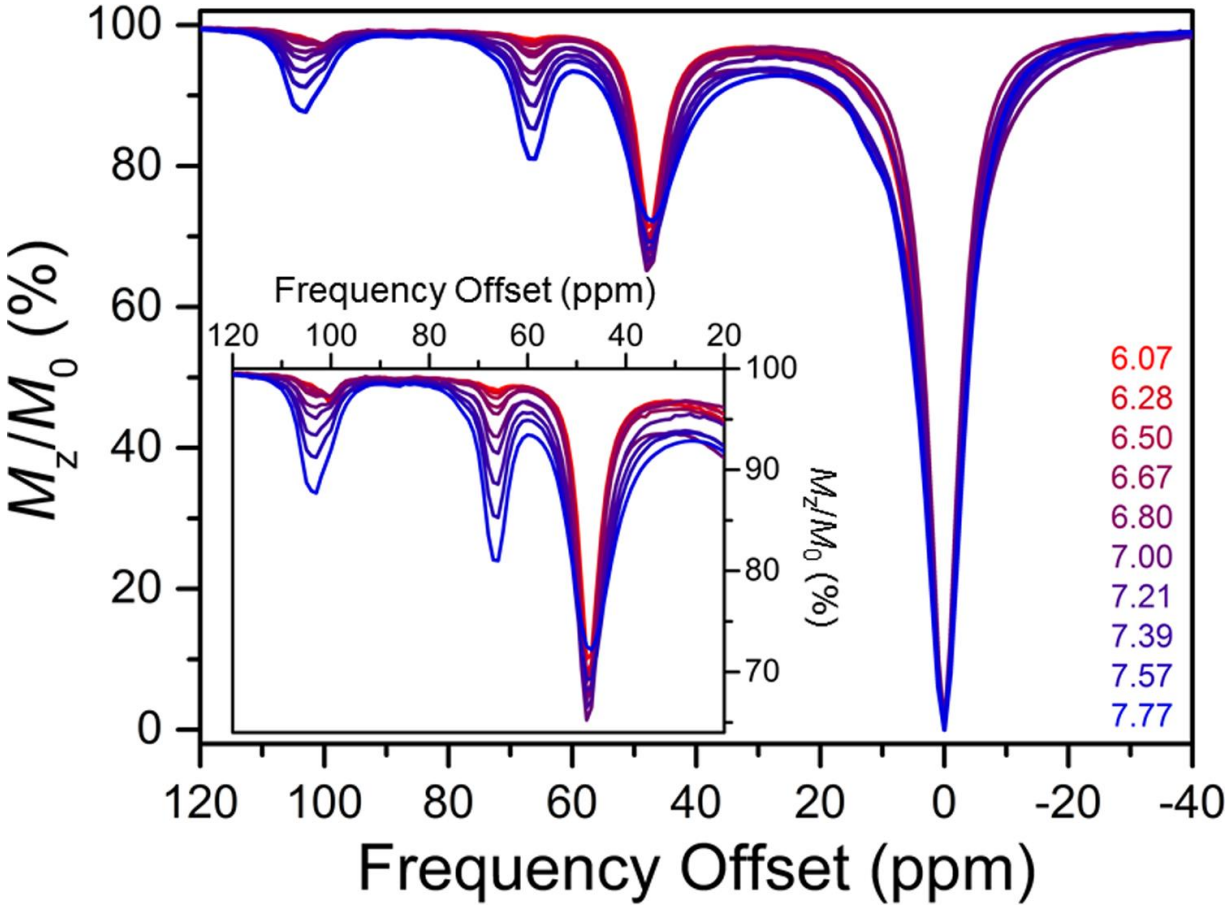

Figure S11 | Variable-pH CEST spectra collected at 11.7 T and 37 °C using 2 s presaturation pulse and B_1 = 22 μT for 5 mM of **3** in aqueous solutions containing 50 mM HEPES and 100 mM NaCl buffered to pH 6.07–7.77 (red to blue). Colored numbers in the legend denote the pH of the solutions measured with a pH electrode and the corresponding color for each sample. Inset: Expanded view of the CEST peaks of interest.

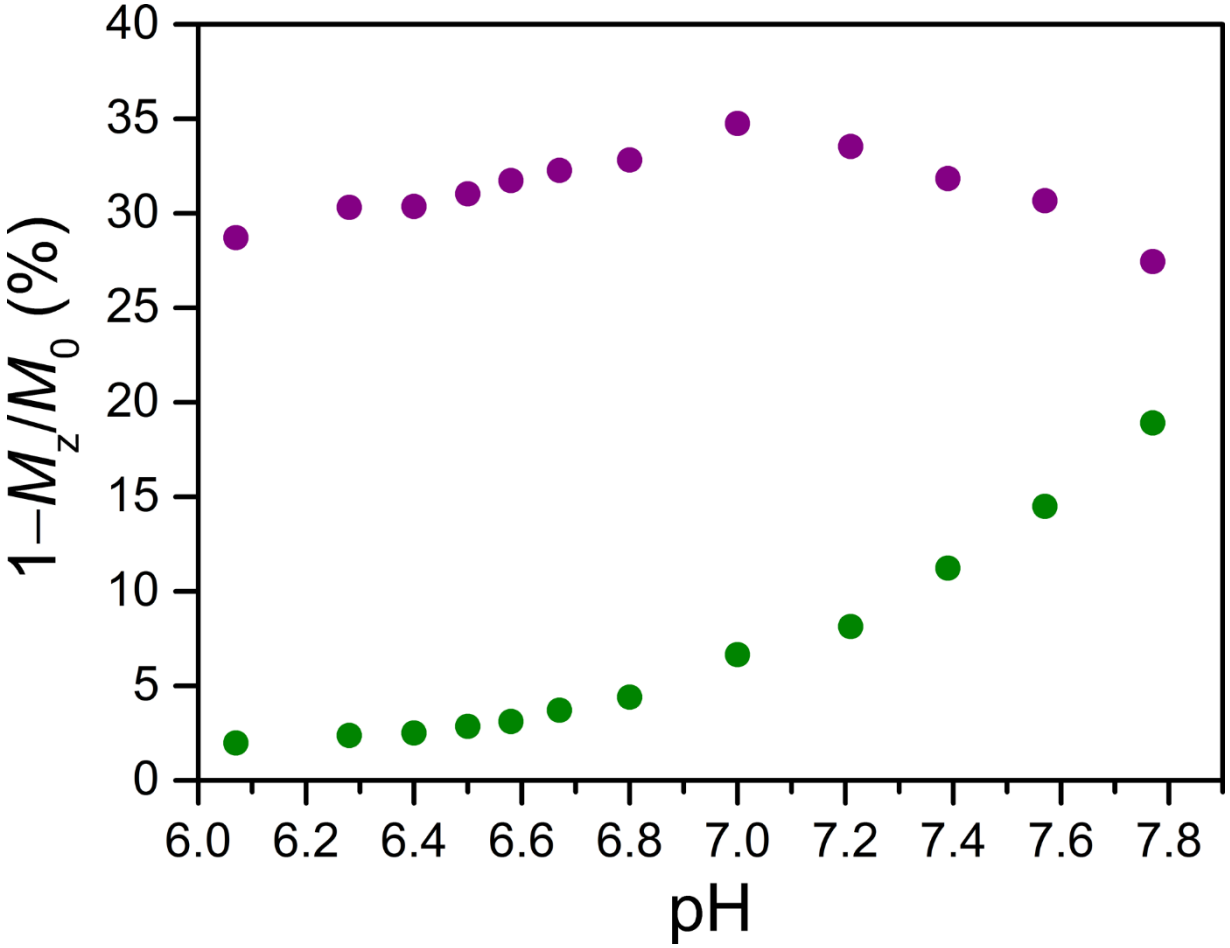

Figure S12 | pH dependences of the CEST intensities from application of 2 s presaturation at 48 ppm (purple) and 67 ppm (green) using B_1 = 22 μT for 5 mM of **3** in aqueous solutions containing 50 mM HEPES and 100 mM NaCl, collected at 37 °C and 11.7 T.

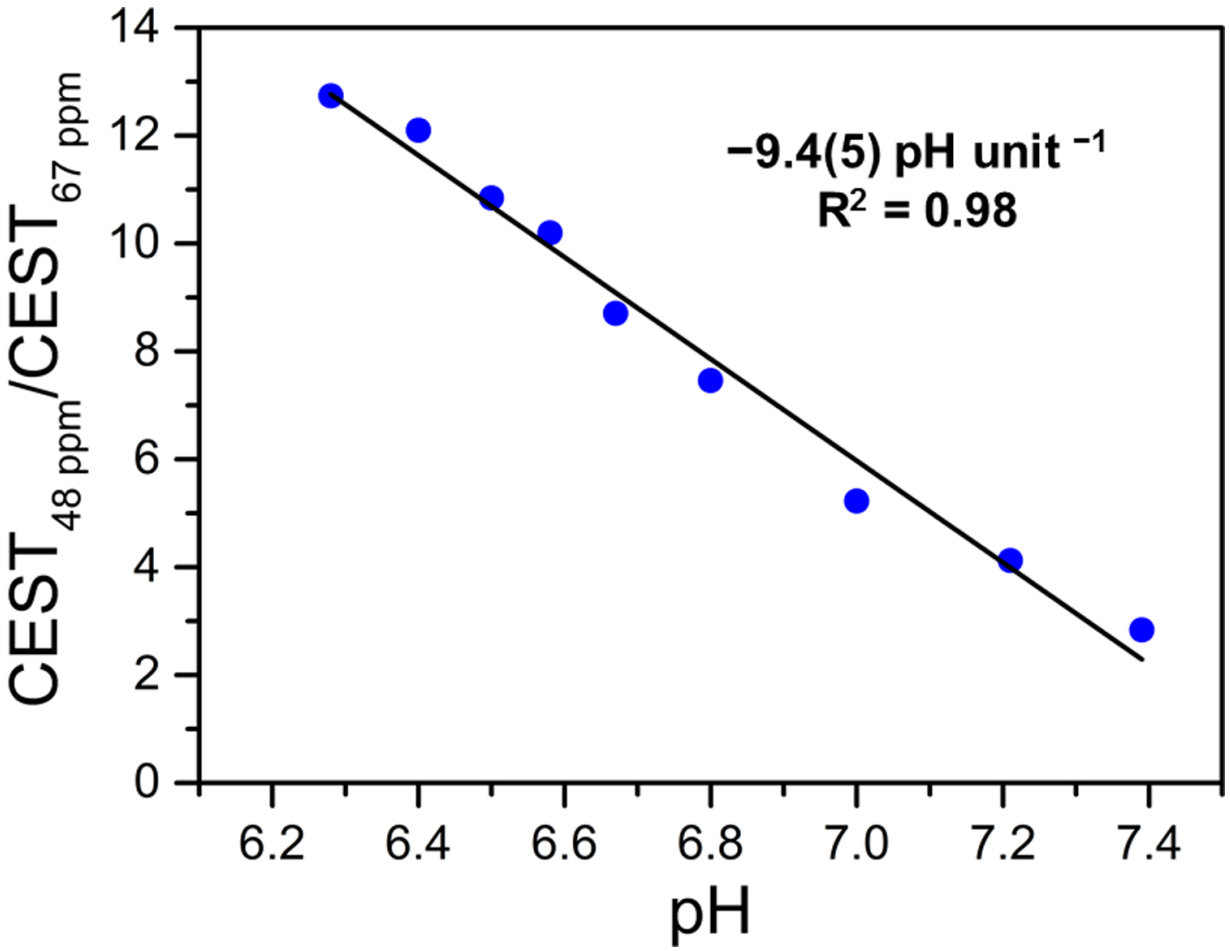

Figure S13 | pH dependence of the ratio of CEST intensities from application of 2 s presaturation at 48 and 67 ppm using B_1 = 22 μT for 5 mM of **3** in aqueous solutions containing 50 mM HEPES and 100 mM NaCl, collected at 37 °C and 11.7 T. Blue circles represent experimental data and the solid black line denotes a linear fit to the data with the following equation: $CEST_{48\ ppm}/CEST_{67\ ppm} = -9.4(5) \times pH + 72(3)$; $R^2 = 0.98$.

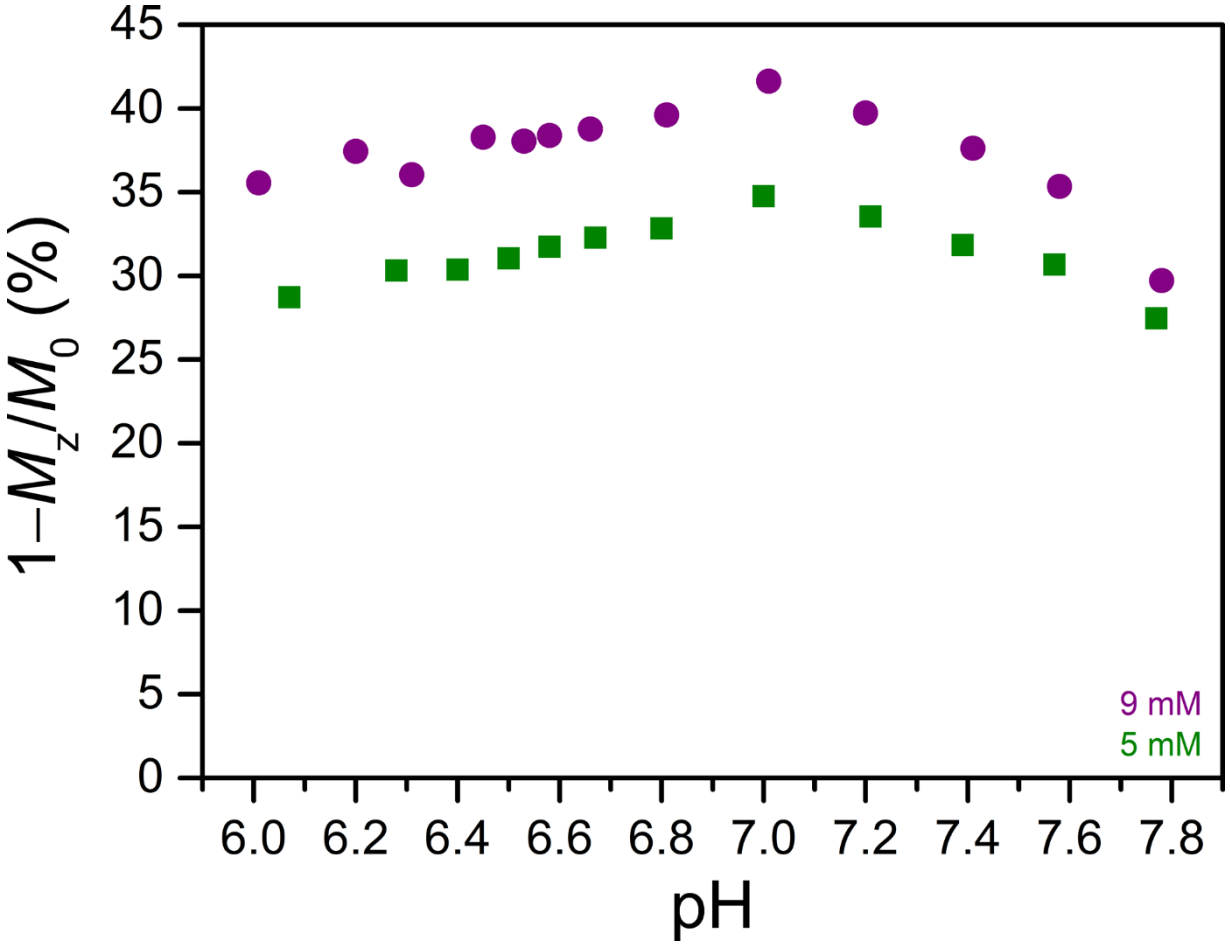

Figure S14 | Comparison of the pH dependence of the CEST intensity from application of 2 s presaturation at 48 ppm using B_1 = 22 μT for different concentrations of **3** (see legend) in aqueous solutions containing 50 mM HEPES and 100 mM NaCl, collected at 37 °C and 11.7 T.

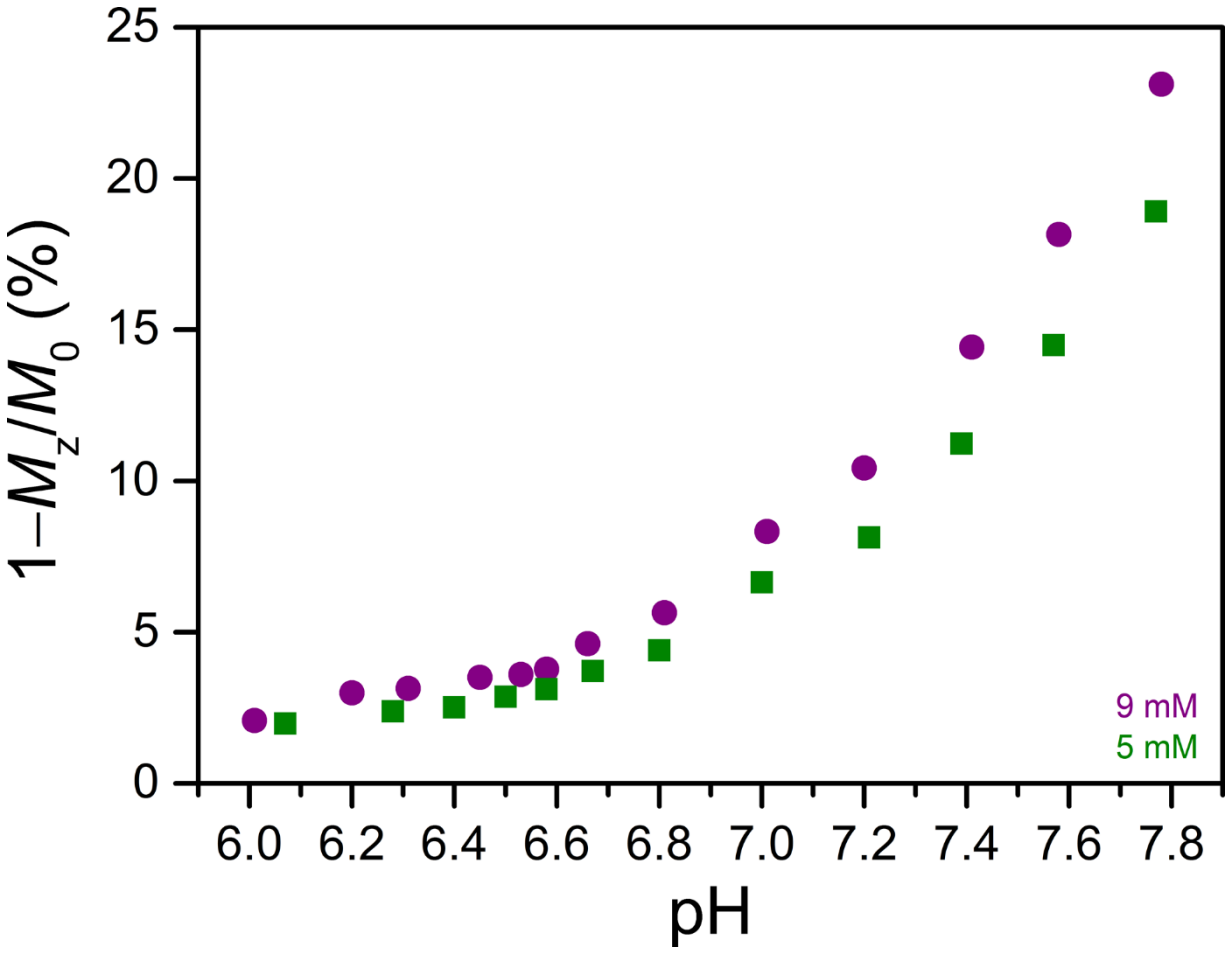

Figure S15 | Comparison of the pH dependence of the CEST intensity from application of 2 s presaturation at 67 ppm using B_1 = 22 μT for different concentrations of **3** (see legend) in aqueous solutions containing 50 mM HEPES and 100 mM NaCl, collected at 37 °C and 11.7 T.

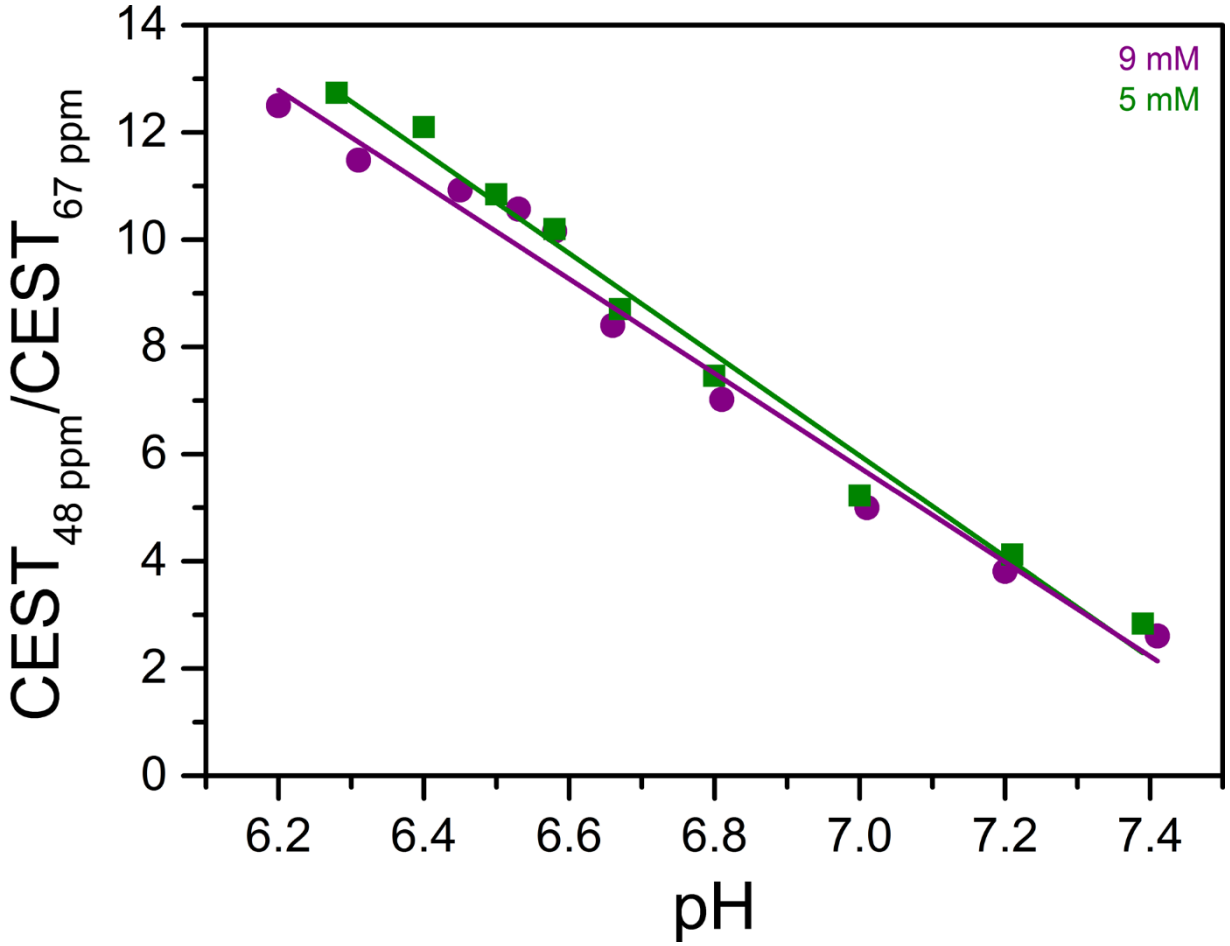

Figure S16 | Comparison of the pH calibration curves obtained by taking the ratios of the CEST intensities from application of 2 s presaturation at 48 and 67 ppm using B_1 = 22 μT for different concentrations of **3** (see legend) in aqueous solutions containing 50 mM HEPES and 100 mM NaCl, collected at 37 °C and 11.7 T. Symbols represent experimental data and solid lines denote linear fits to the data with the following equations: (9 mM) $CEST_{48\ ppm}/CEST_{67\ ppm} = -8.8(5) \times pH + 67(4)$, R^2 = 0.98; (5 mM) $CEST_{48\ ppm}/CEST_{67\ ppm} = -9.4(5) \times pH + 72(3)$, R^2 = 0.98.

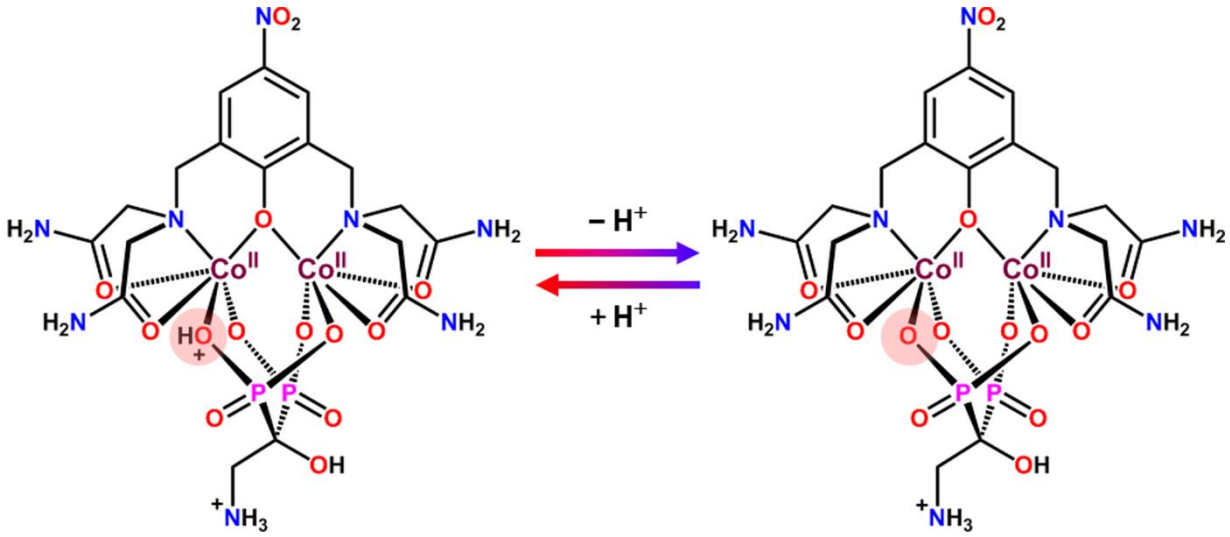

Figure S17 | Scheme highlighting the ionization process taking place on the ancillary bisphosphonate ligand for the dicobalt complex in **3**, in the pH range 1.50–7.80.

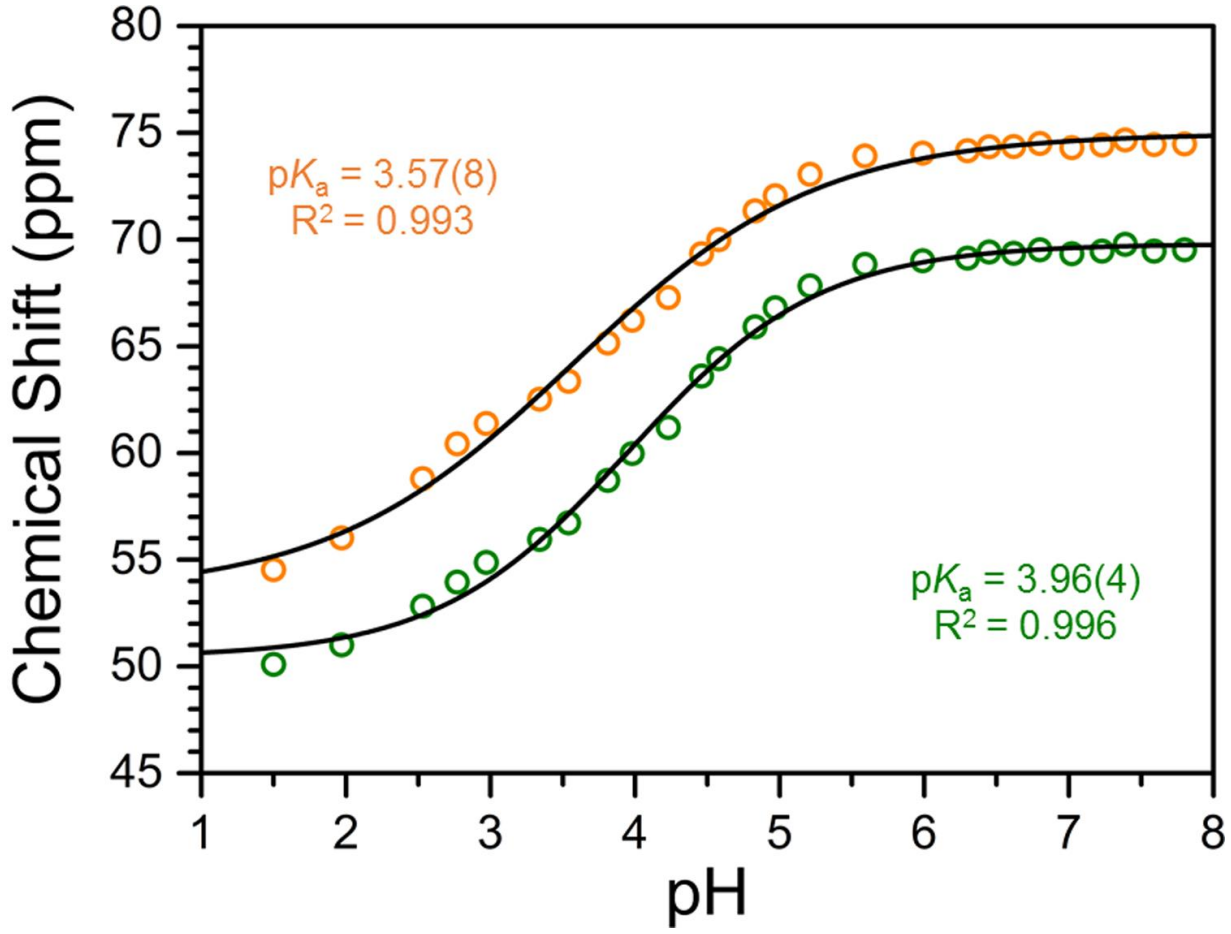

Figure S18 | pH dependences of the ^{1}H NMR chemical shifts (reported as frequency offsets) of the two inequivalent methylene proton resonances from the ancillary bisphosphonate ligand for **3** in aqueous solutions containing 50 mM HEPES and 100 mM NaCl, collected at 37 °C and 11.7 T. Circles represent experimental data and solid lines correspond to sigmoidal fits to the data (see Equation 1 in the Experimental Section). Fits to the data give pK_a = 3.57(8) (R^2 = 0.993) and 3.96(4) (R^2 = 0.996) for the two methylene proton resonances, respectively. The ionization process taking place on the ancillary bisphosphonate is highlighted with the schematics of the complex in Figure S17.

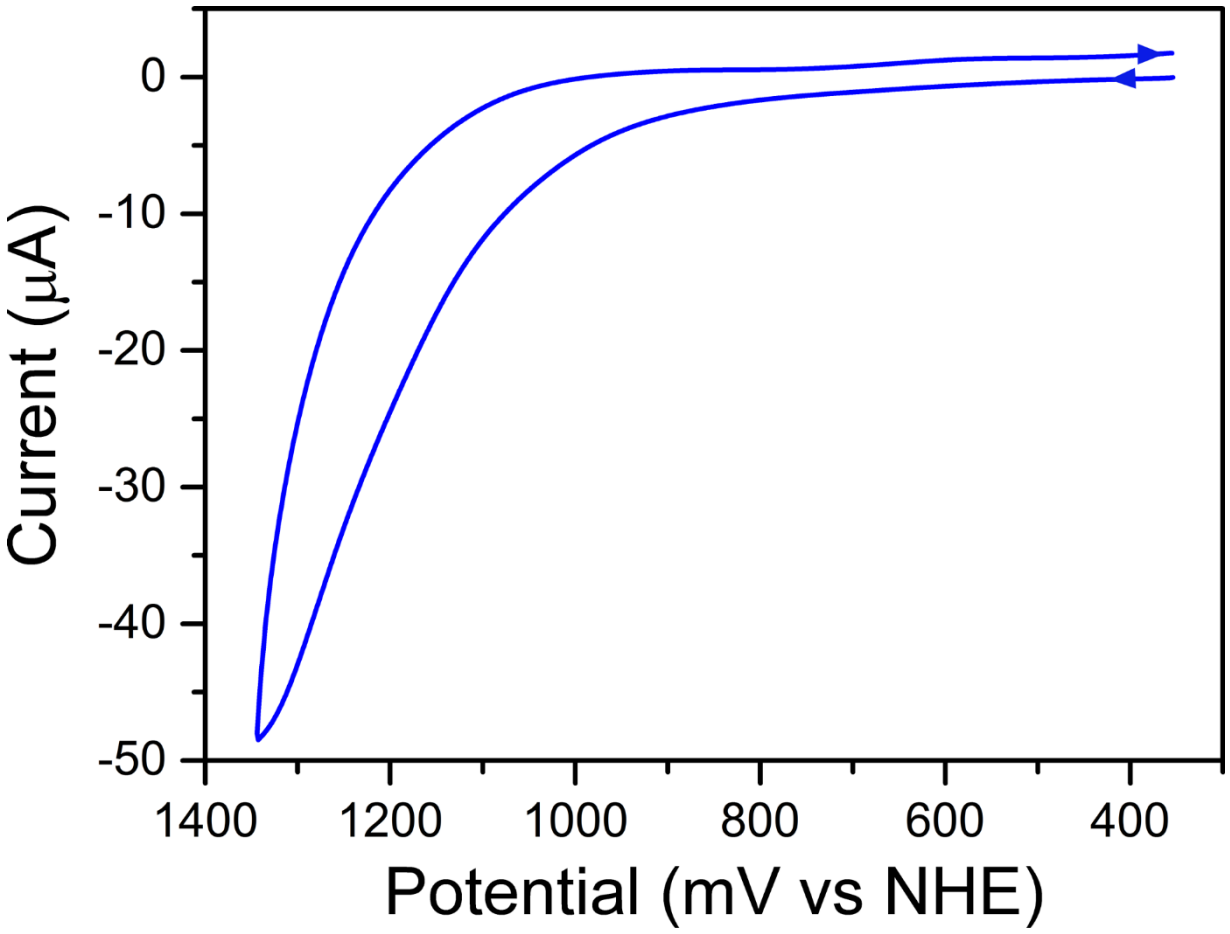

Figure S19 | Cyclic voltammogram for 2 mM of **3** in an aqueous solution containing 50 mM HEPES and 100 mM NaCl buffered to pH 7.4. Measurements were carried out at ambient temperature using a glassy carbon electrode as a working electrode and 20 mV s^{-1} scan rate. The blue arrows denote the scan direction.

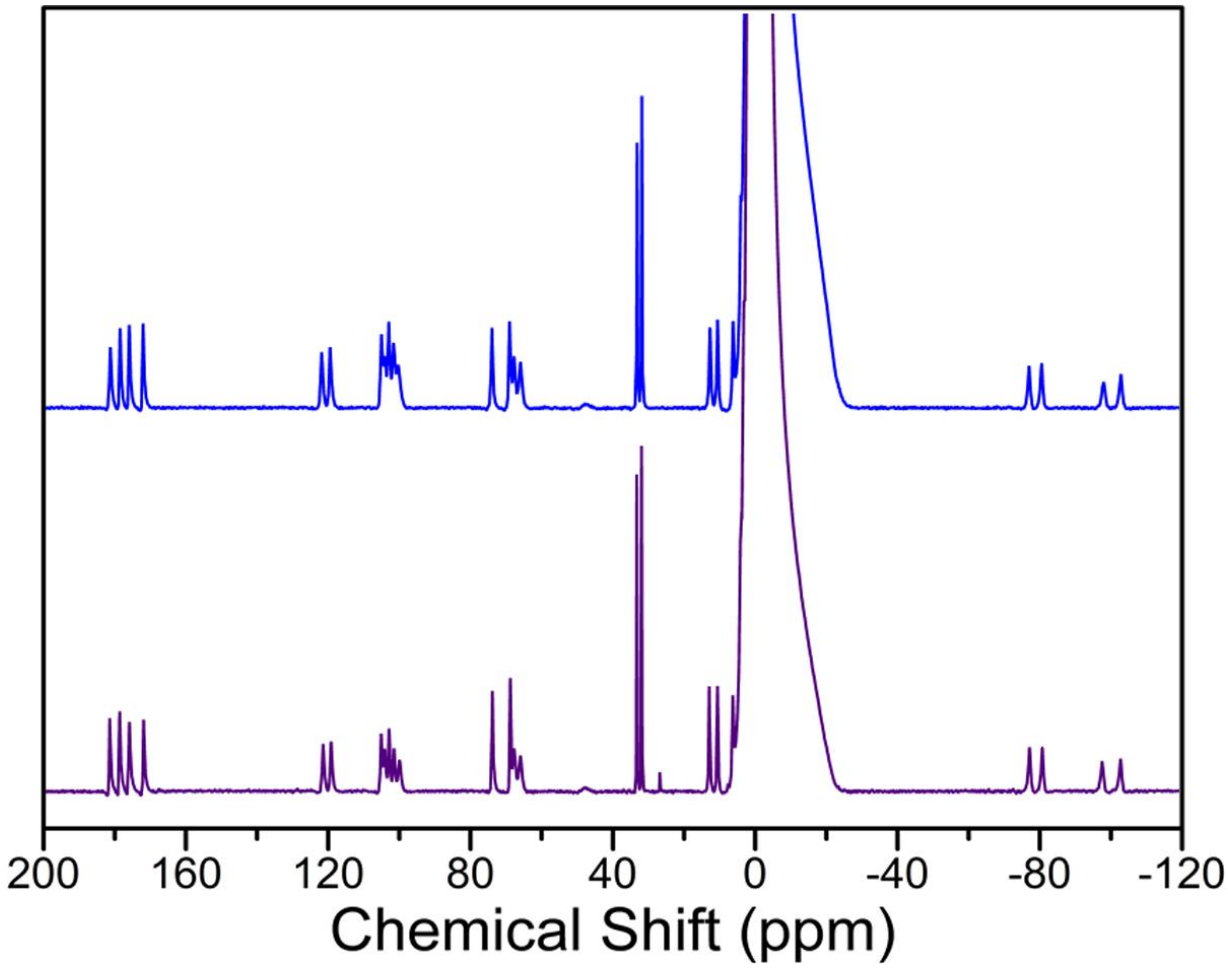

Figure S20 | Stacked ^{1}H NMR spectra of 9 mM of **3** in an aqueous solution containing 50 mM HEPES and 100 mM NaCl buffered to pH 7.4 without (blue) and with (purple) the presence of 9 mM of each NaH_2PO_4, Na_3ADP ($(ADP)^{3-}$ = adenosine 5′-diphosphate), and Na_2H_2ATP ($(ATP)^{4-}$ = adenosine 5′-triphosphate), collected at 37 °C and 14.1 T. Note that compound **3** was incubated with the solution of the phosphate ions at 25 °C for 24 h prior to the NMR experiment.

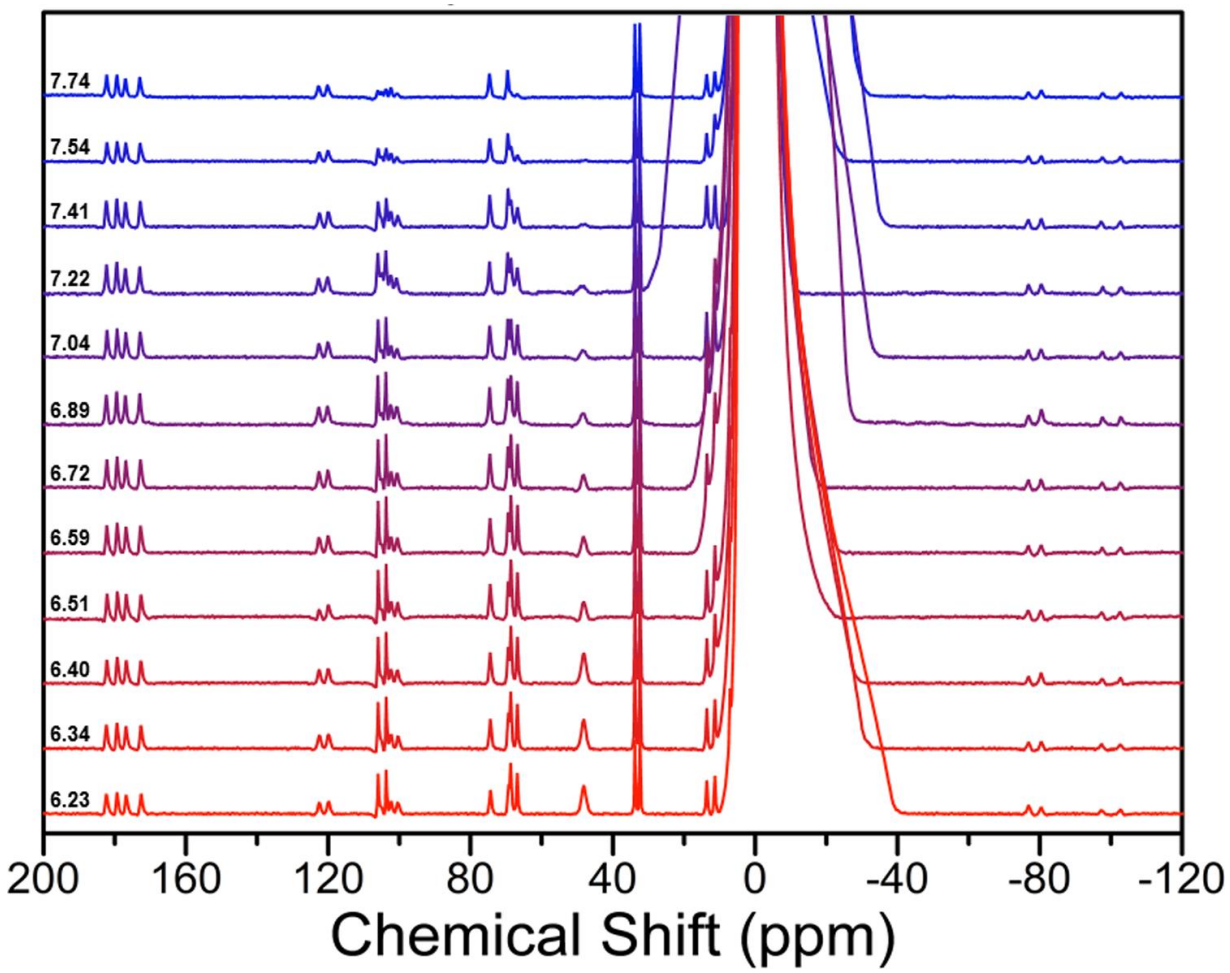

Figure S21 | Variable-pH ^{1}H NMR spectra of 8 mM of **3** in FBS at various pH values, collected at 37 °C and 14.1 T. Black numbers on the left denote the pH of the NMR sample solutions measured with a pH electrode.

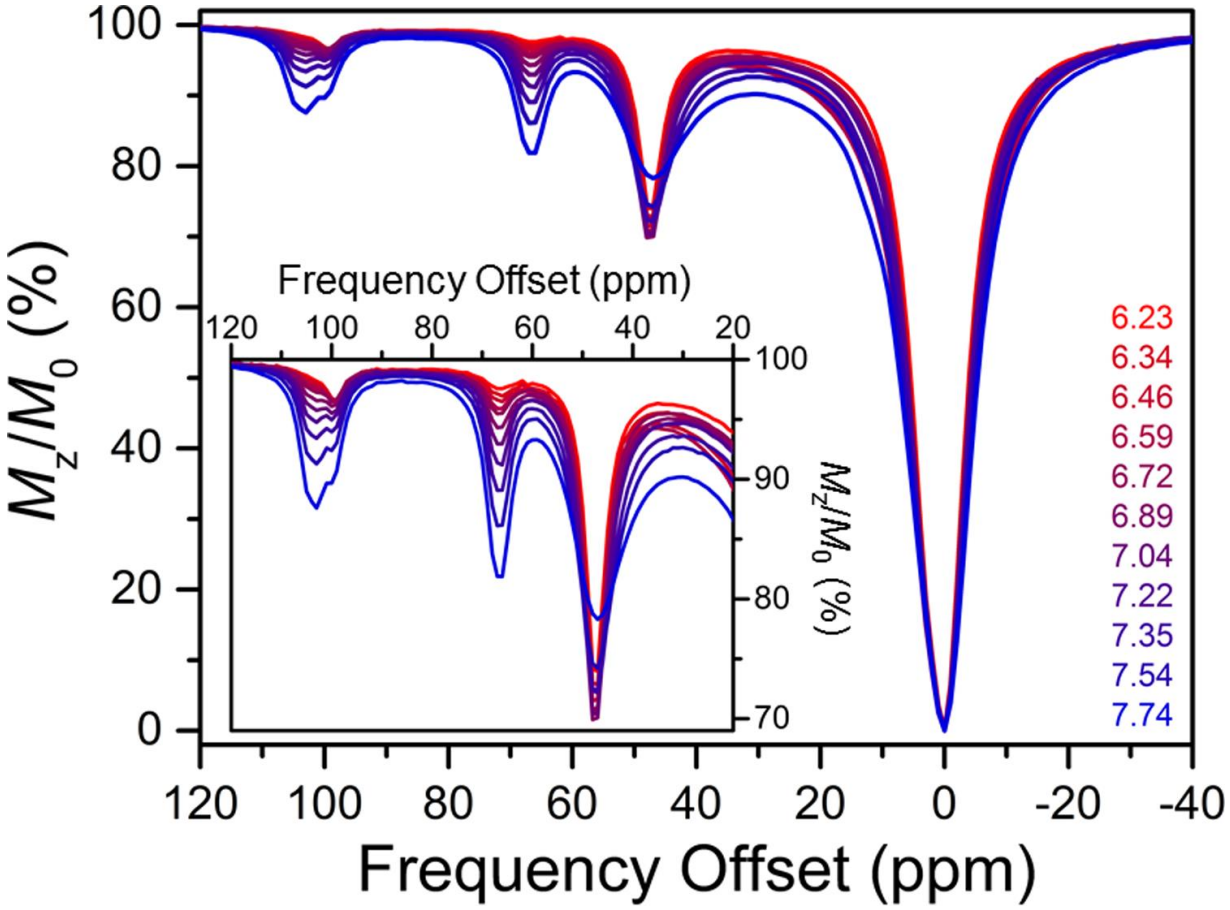

Figure S22 | Variable-pH CEST spectra collected at 11.7 T and 37 °C using 2 s presaturation pulse and B_1 = 22 μT for 8 mM of **3** in FBS at pH 6.23–7.74 (red to blue). Colored numbers in the legend denote the pH of the solutions measured with a pH electrode and the corresponding color for each sample. Inset: Expanded view of the CEST peaks of interest.

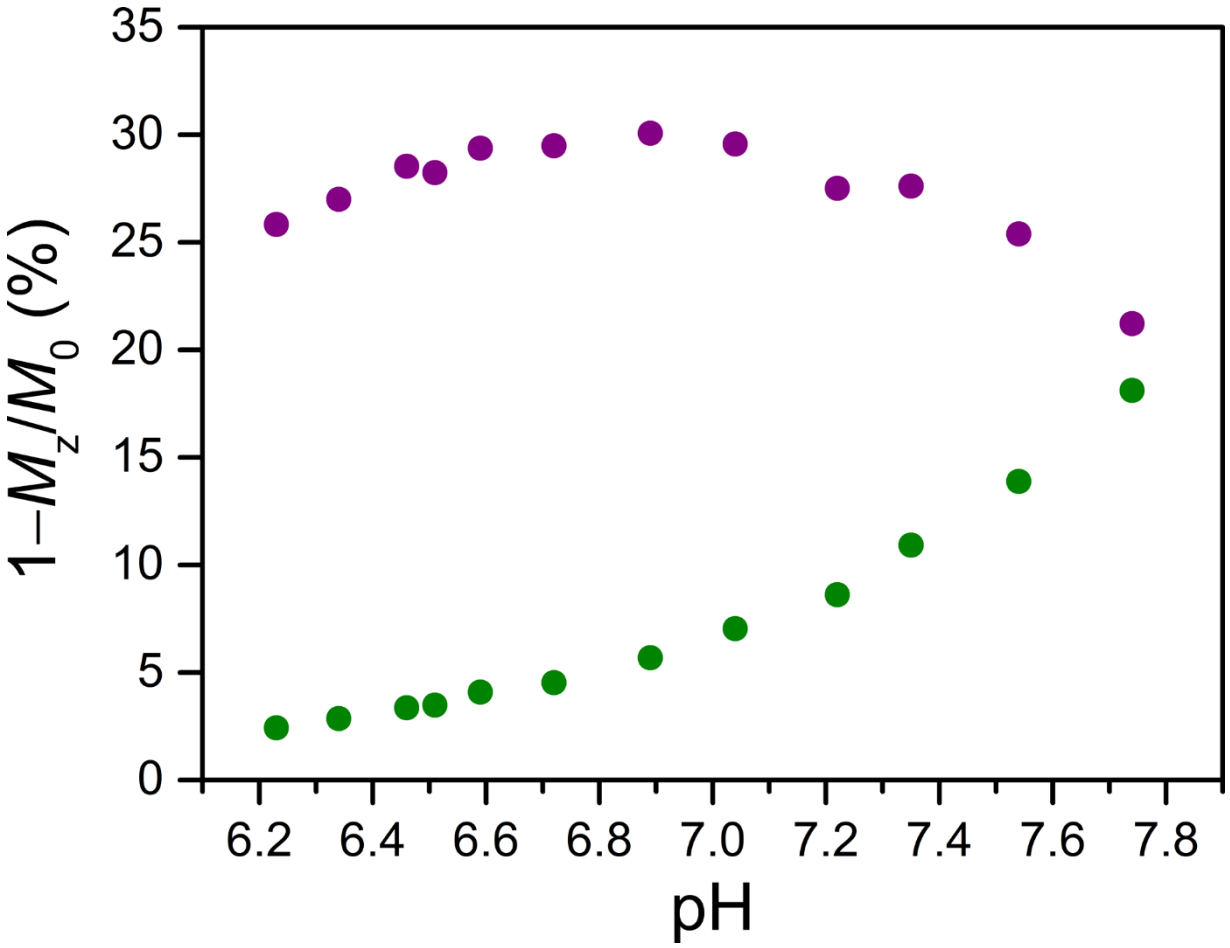

Figure S23 | pH dependences of the CEST intensities from application of 2 s presaturation at 48 ppm (purple) and 67 ppm (green) using B_1 = 22 μT for 8 mM of **3** in FBS, collected at 37 °C and 11.7 T.

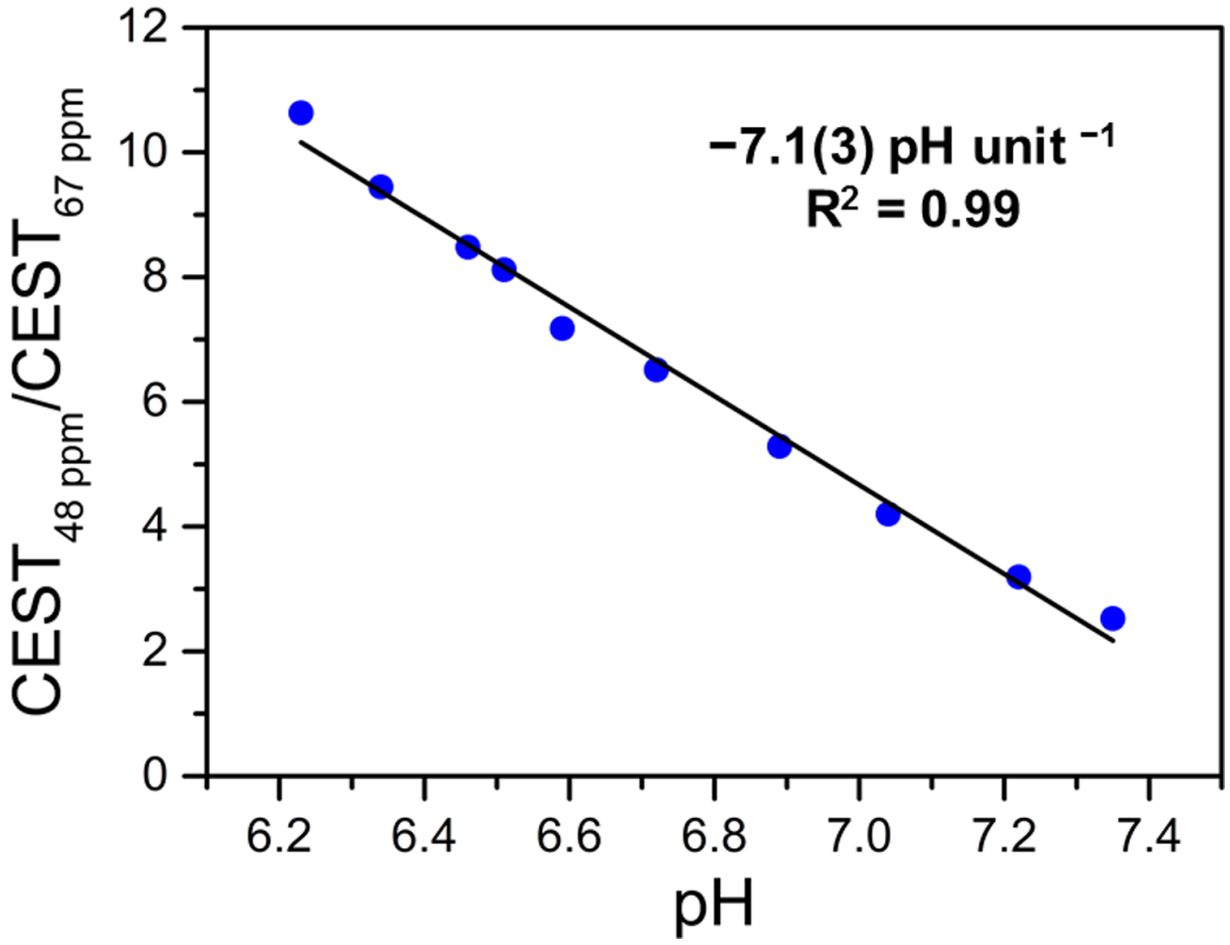

Figure S24 | pH dependence of the ratio of CEST intensities from application of 2 s presaturation at 48 and 67 ppm using B_1 = 22 μT for 8 mM of **3** in FBS, collected at 37 °C and 11.7 T. Blue circles represent experimental data and the solid black line denotes a linear fit to the data with the following equation: $CEST_{48\ ppm}/CEST_{67\ ppm} = -7.1(3) \times pH + 55(2)$; $R^2 = 0.99$.

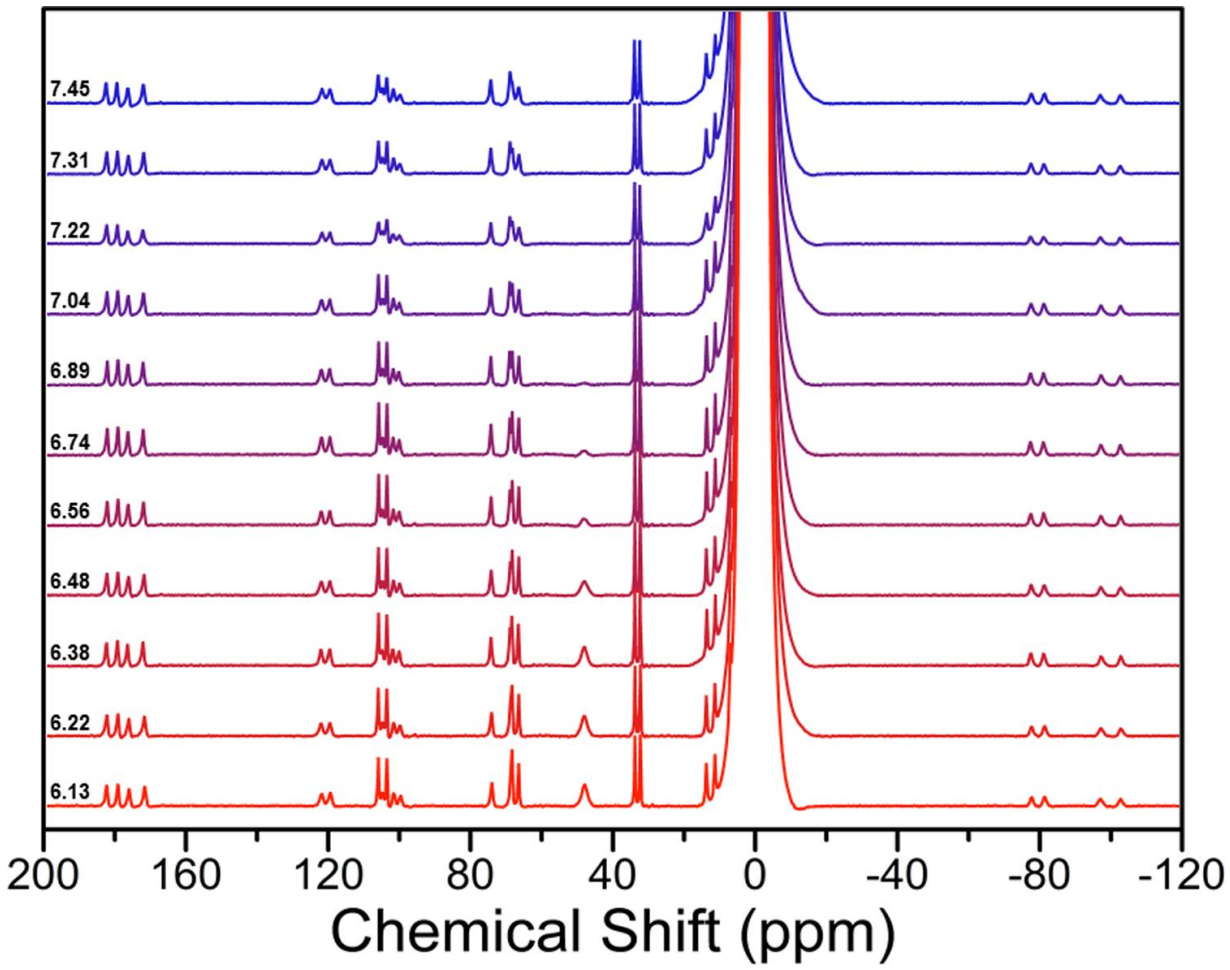

Figure S25 | Variable-pH ^{1}H NMR spectra of 8 mM of **3** in 17% (w/v) gelatin gels at various pH values, collected at 37 °C and 14.1 T. Black numbers on the left denote the pH of the NMR samples measured with a pH electrode.

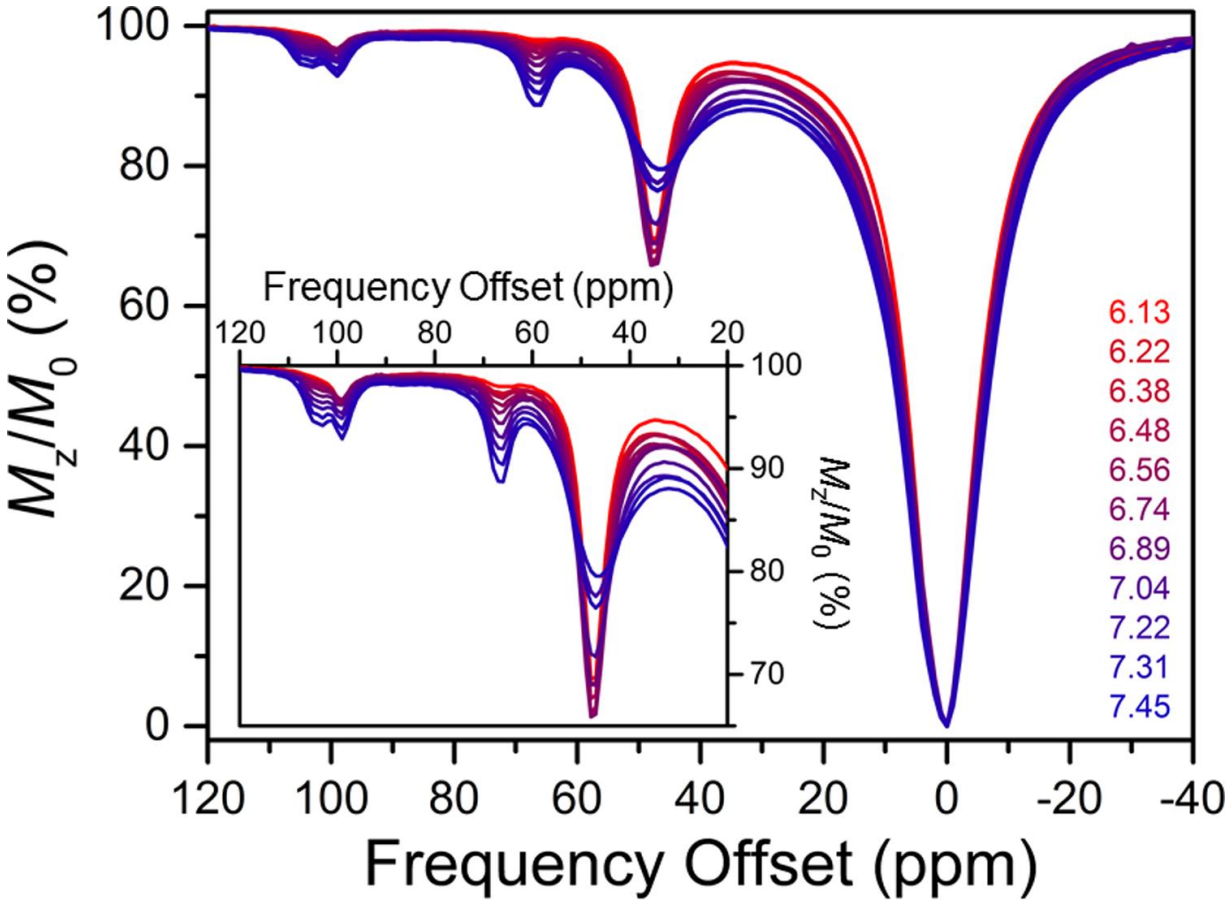

Figure S26 | Variable-pH CEST spectra collected at 11.7 T and 37 °C using 2 s presaturation pulse and B_1 = 22 μT for 8 mM of **3** in 17% (w/v) gelatin gels at pH 6.13–7.45 (red to dark purple). Colored numbers in the legend denote the pH of the samples measured with a pH electrode and the corresponding color for each sample. Inset: Expanded view of the CEST peaks of interest.

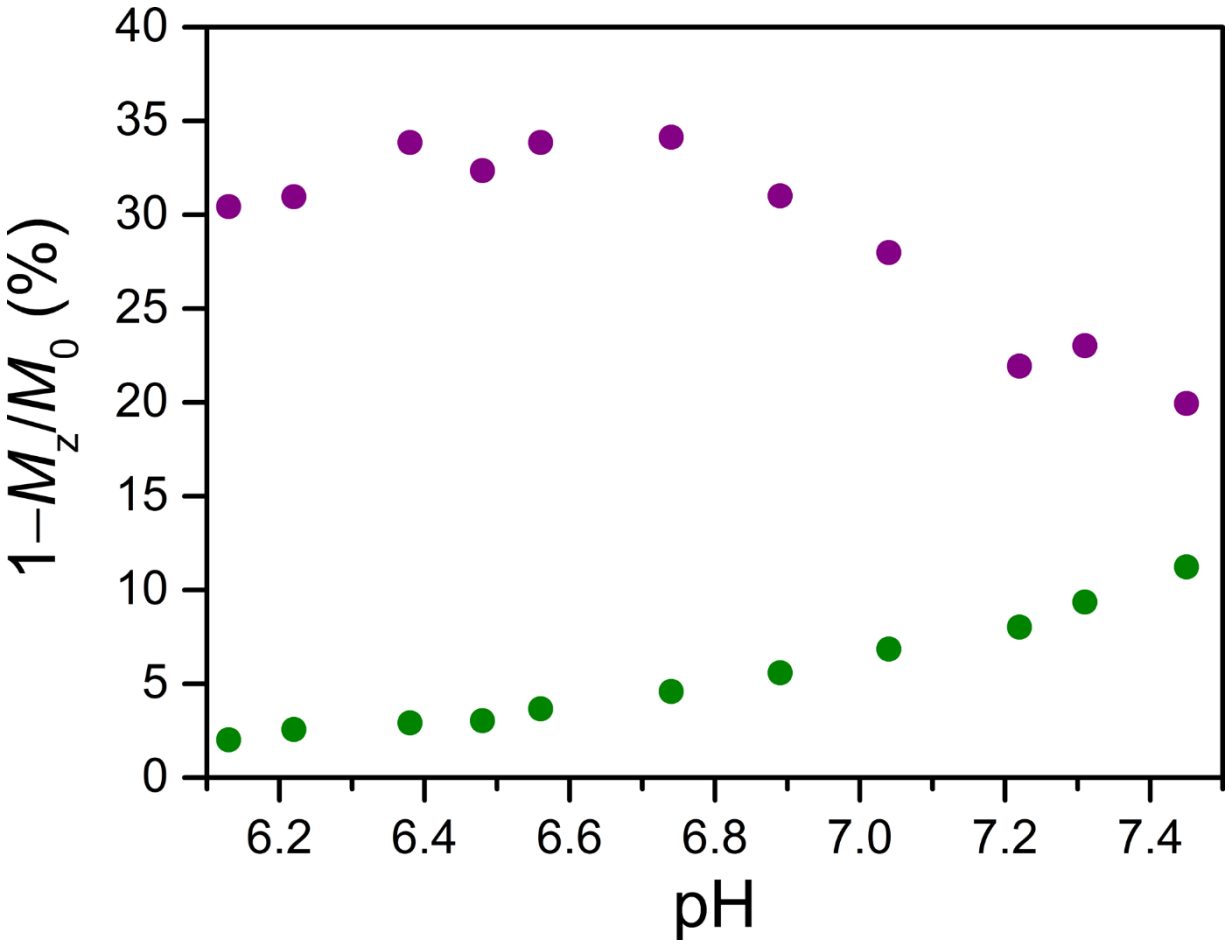

Figure S27 | pH dependences of the CEST intensities from application of 2 s presaturation at 48 ppm (purple) and 67 ppm (green) using B_1 = 22 μT for 8 mM of **3** in 17% (w/v) gelatin gels, collected at 37 °C and 11.7 T.

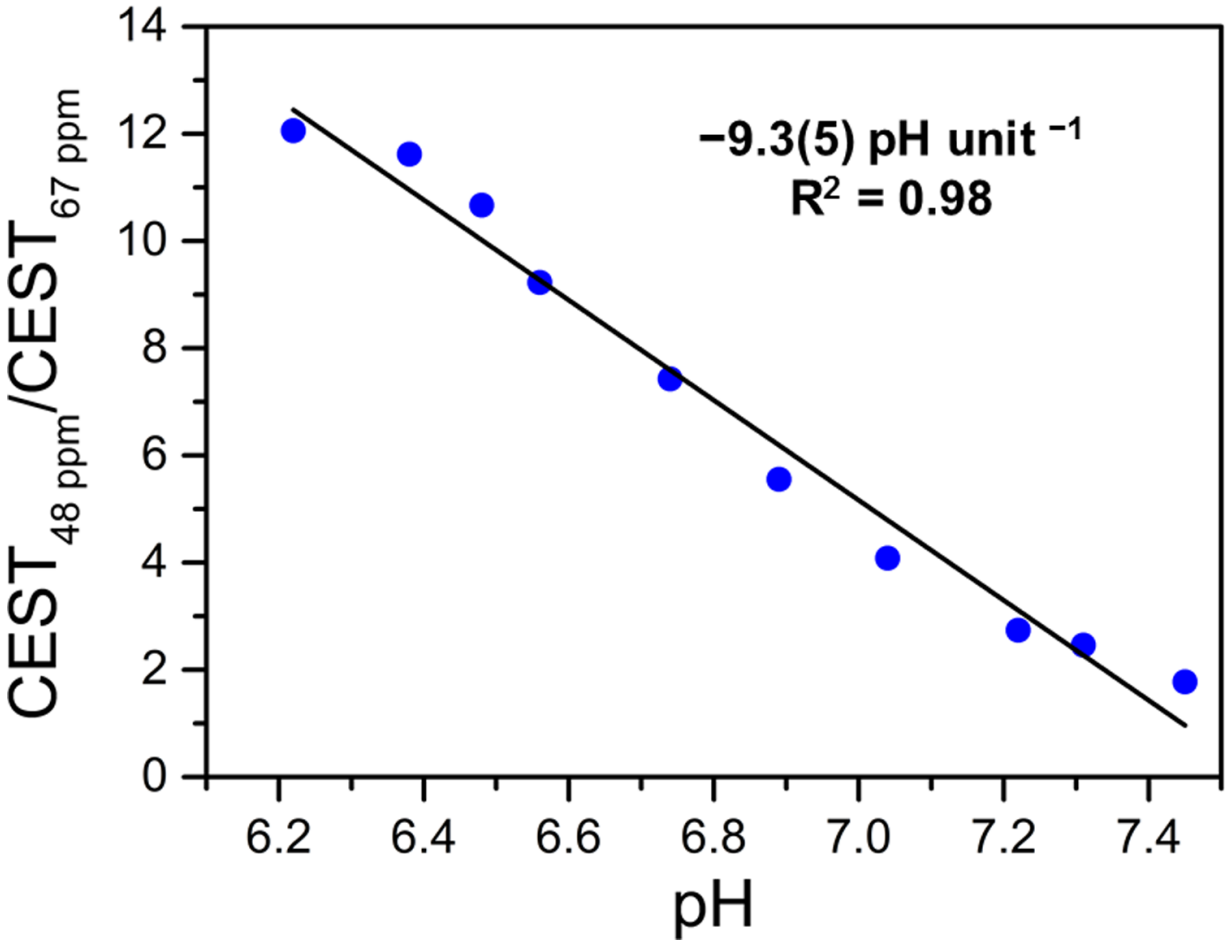

Figure S28 | pH dependence of the ratio of CEST intensities from application of 2 s presaturation at 48 and 67 ppm using B_1 = 22 μT for 8 mM of **3** in 17% (w/v) gelatin gels, collected at 37 °C and 11.7 T. Blue circles represent experimental data and the solid black line denotes a linear fit to the data with the following equation: $CEST_{48\ ppm}/CEST_{67\ ppm} = -9.3(5) \times pH + 71(4)$; $R^2 = 0.98$.

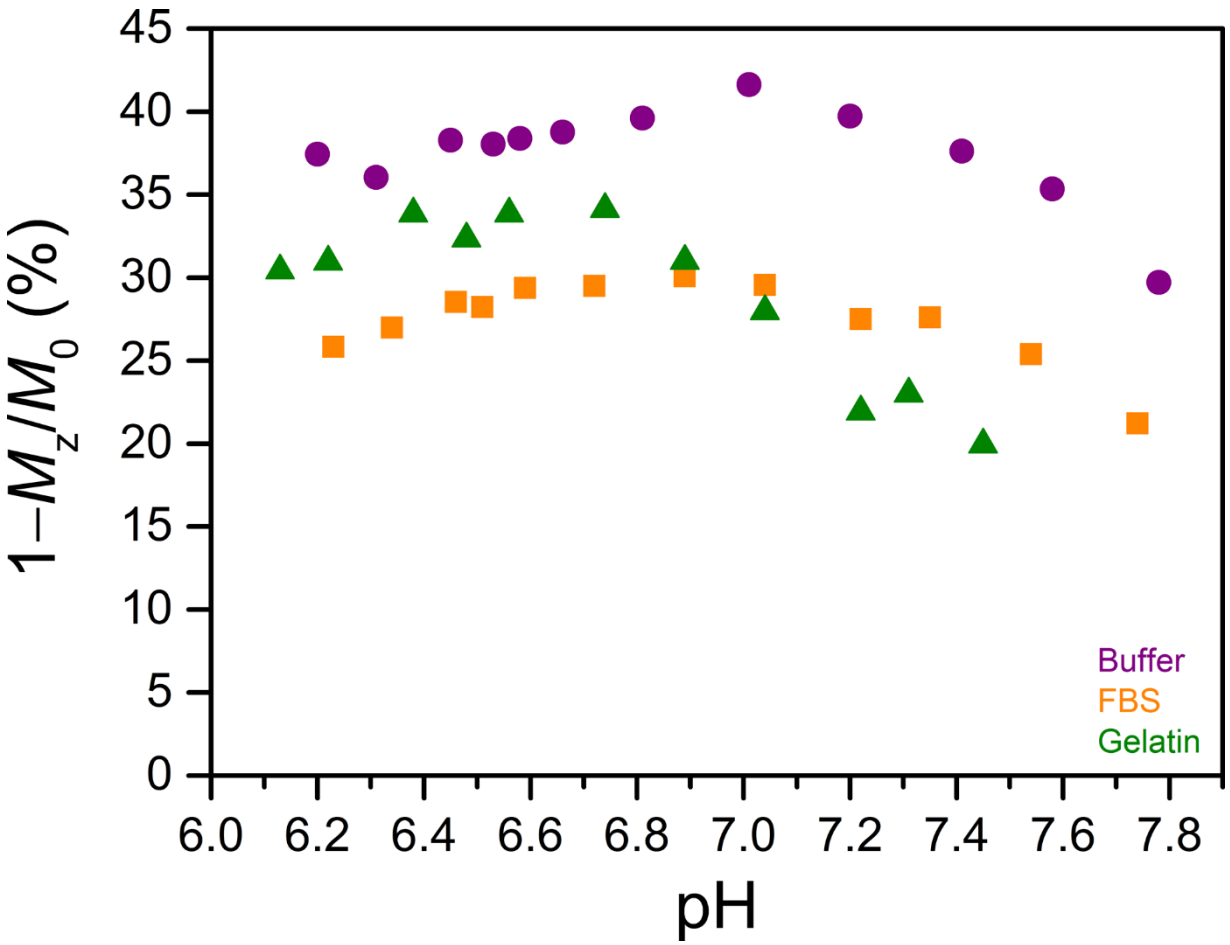

Figure S29 | Comparison of the pH dependence of the CEST intensity from application of 2 s presaturation at 48 ppm using B_1 = 22 μT for **3** in aqueous buffer solutions containing 50 mM HEPES and 100 mM NaCl (purple; 9 mM), in FBS (orange; 8 mM), and in 17% (w/v) gelatin gels (green; 8 mM), collected at 37 °C and 11.7 T.

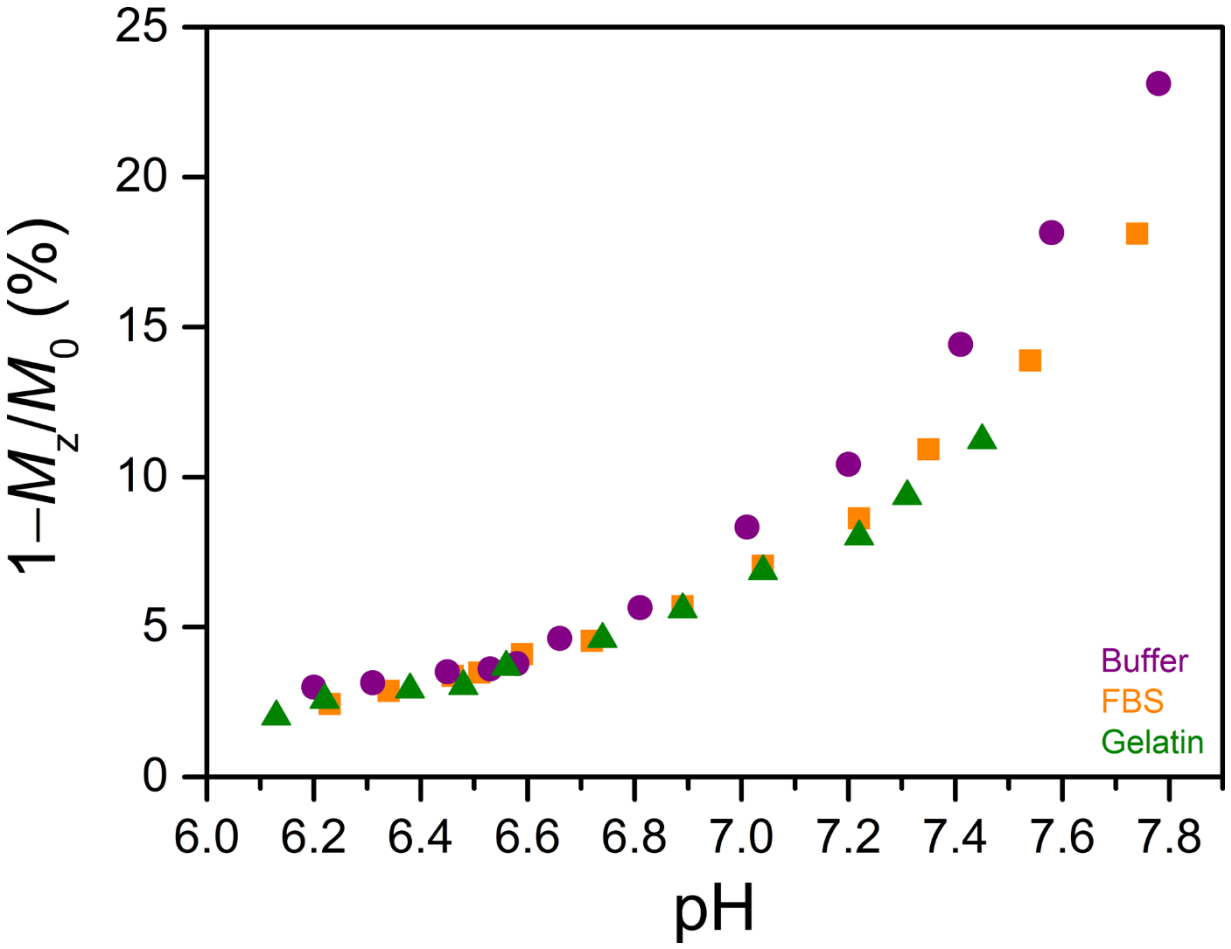

Figure S30 | Comparison of the pH dependence of the CEST intensity from application of 2 s presaturation at 67 ppm using B_1 = 22 μT for **3** in aqueous buffer solutions containing 50 mM HEPES and 100 mM NaCl (purple; 9 mM), in FBS (orange; 8 mM), and in 17% (w/v) gelatin gels (green; 8 mM), collected at 37 °C and 11.7 T.

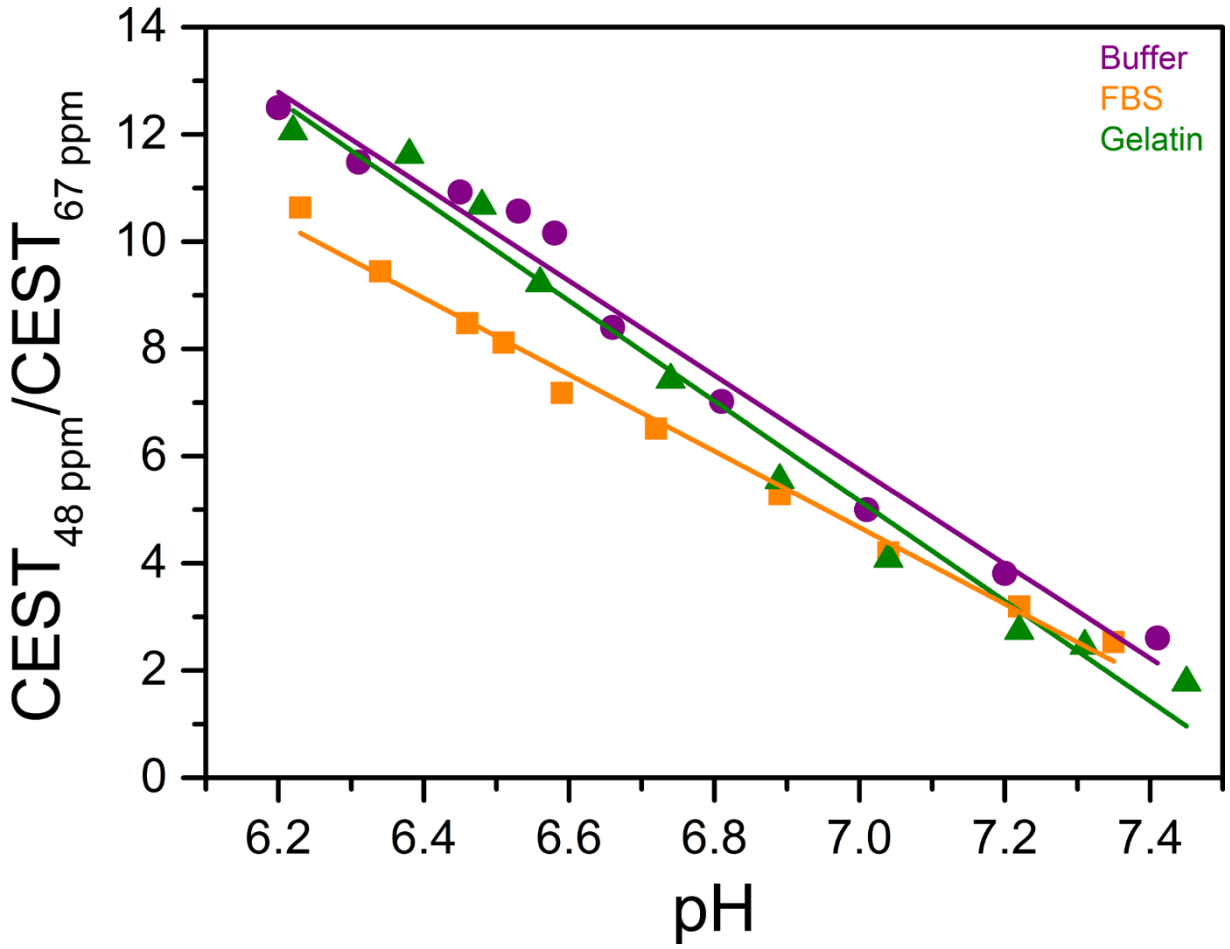

Figure S31 | Comparison of the pH calibration curves obtained by taking the ratios of the CEST intensities from application of 2 s presaturation at 48 and 67 ppm using B_1 = 22 μT for **3** in aqueous buffer solutions containing 50 mM HEPES and 100 mM NaCl (purple), in FBS (orange), and in 17% (w/v) gelatin gels (green), collected at 37 °C and 11.7 T. See manuscript and Figures S24 and S28 for the equations of the linear fits to the data.

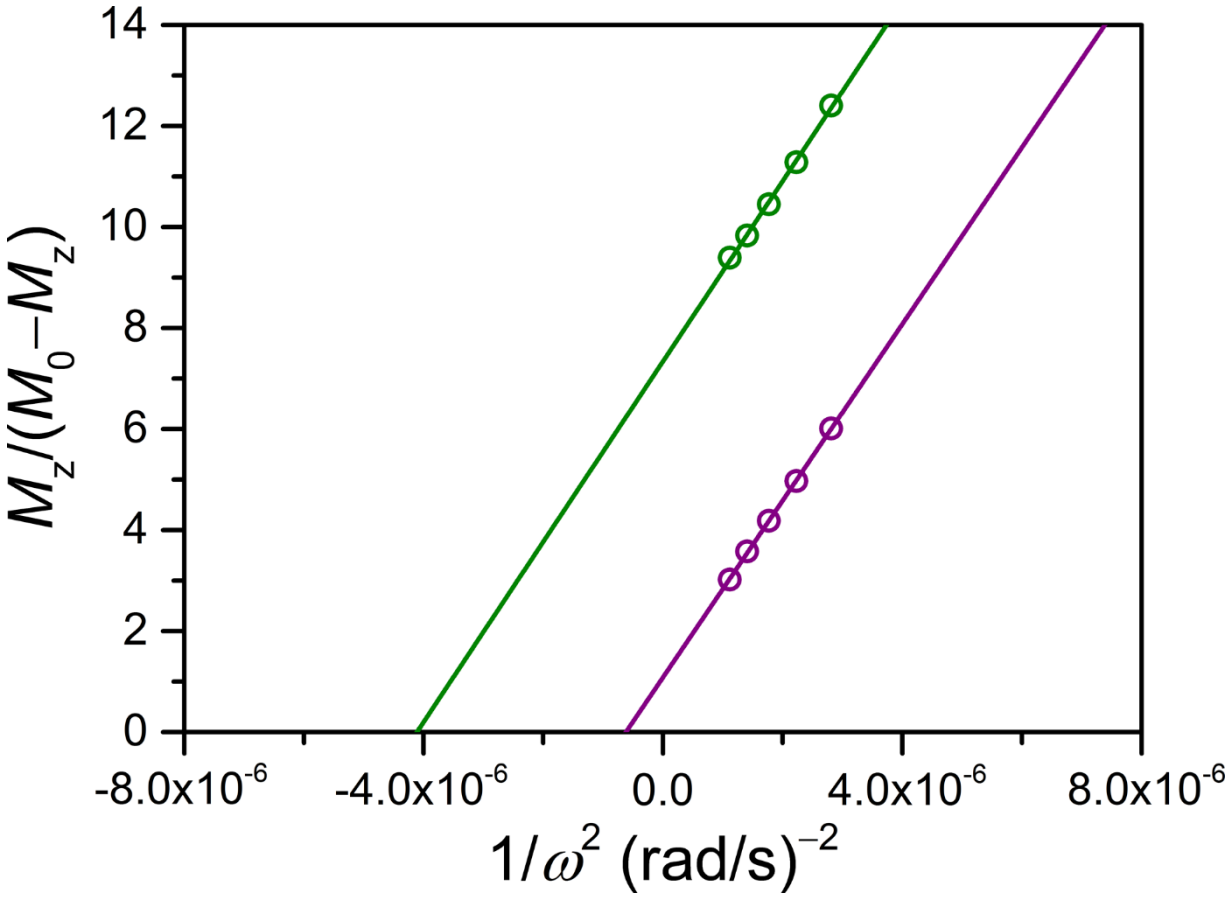

Figure S32 | Omega plots of the CEST effects from application of 6 s presaturation at 48 ppm (purple) and 67 ppm (green) using B_1 = 14–22 μT for 8 mM of **3** in FBS at pH 7.46, collected at 37 °C and 11.7 T. Circles represent experimental data and lines represent linear fits to the data.

Table S2 | Comparison of proton exchange rate constants (k_{ex}) for **3** in an aqueous solution containing 50 mM HEPES and 100 mM NaCl buffered to pH 7.41 and in FBS at pH 7.46, obtained from Omega plots at 37 °C and 11.7 T.

	48 ppm	**67 ppm**
pH 7.41 buffer	$1.26(4) \times 10^3\ s^{-1}$	$4.4(2) \times 10^2\ s^{-1}$
pH 7.46 FBS	$1.27(3) \times 10^3\ s^{-1}$	$4.9(1) \times 10^2\ s^{-1}$

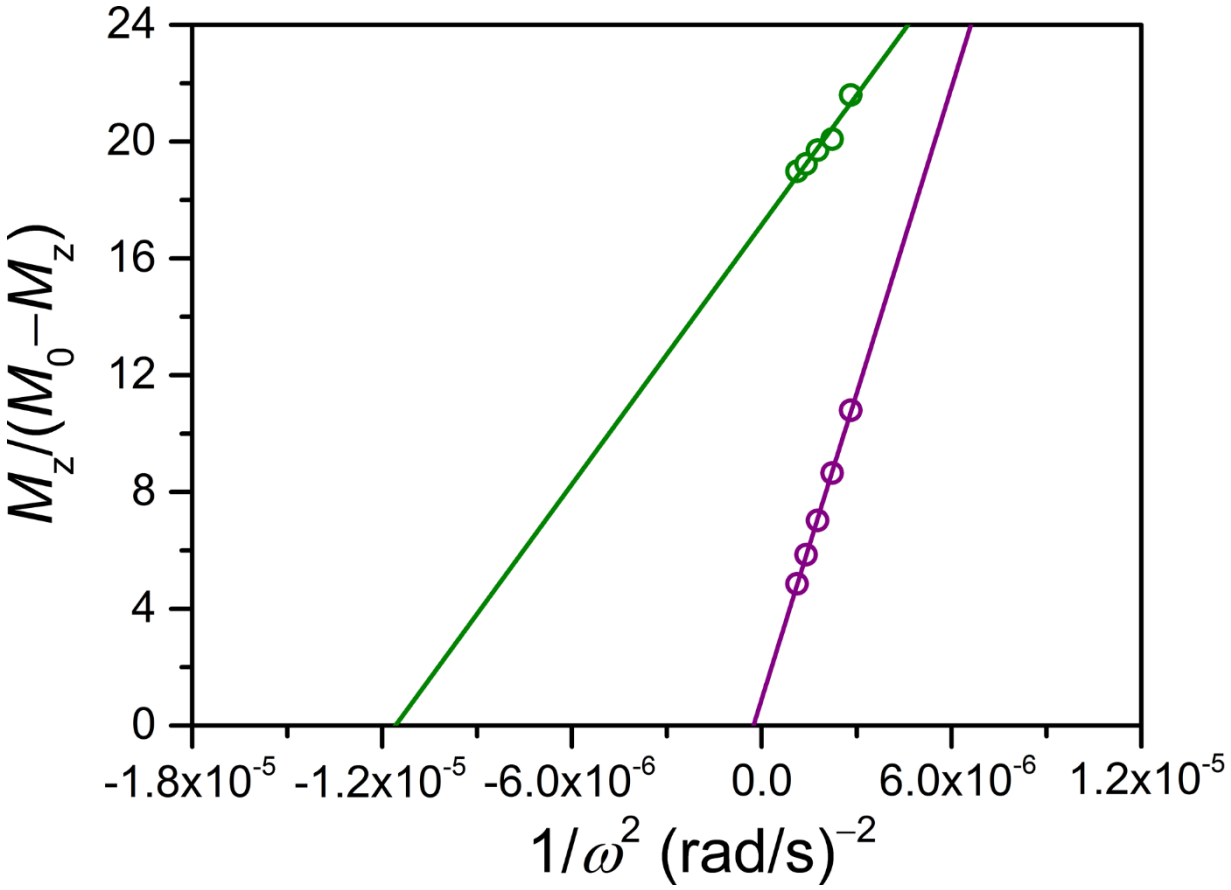

Figure S33 | Omega plots of the CEST effects from application of 6 s presaturation at 48 ppm (purple) and 67 ppm (green) using B_1 = 14–22 μT for 8 mM of **3** in a 17% (w/v) gelatin gel at pH 7.22, collected at 37 °C and 11.7 T. Circles represent experimental data and lines represent linear fits to the data.

Table S3 | Comparison of proton exchange rate constants (k_{ex}) for **3** in an aqueous solution containing 50 mM HEPES and 100 mM NaCl buffered to pH 7.20 and in a 17% (w/v) gelatin gel at pH 7.22, obtained from Omega plots at 37 °C and 11.7 T.

	48 ppm	**67 ppm**
pH 7.20 buffer	$9.9(2) \times 10^2\ s^{-1}$	$4.2(1) \times 10^2\ s^{-1}$
pH 7.22 gelatin	$2.0(2) \times 10^3\ s^{-1}$	$2.9(3) \times 10^2\ s^{-1}$

Table S4 | Comparison of T_1 relaxation times of H_2O at 37 °C and 11.7 T in an aqueous solution containing 50 mM HEPES and 100 mM NaCl buffered to pH 7.35 and in FBS at pH 7.50.

	$\boldsymbol{T_1}$
pH 7.35 buffer	4.2(1) s
pH 7.50 FBS	3.5(1) s

References

(1) A. E. Thorarinsdottir, K. Du, J. H. P. Collins and T. D. Harris, *J. Am. Chem. Soc*., 2017, **139**, 15836–15847.

(2) M. Egorov, S. Aoun, M. Padrines, F. Redini, D. Heymann, J. Lebreton and M. Mathé-Allainmat, *Eur. J. Org. Chem*., 2011, **2011**, 7148–7154.

(3) OriginPro, version 9.0, OriginLab Corp., Northampton, MA, 2003.

(4) W. T. Dixon, J. Ren, A. J. M. Lubag, J. Ratnakar, E. Vinogradov, I. Hancu, R. E. Lenkinski and A. D. Sherry, *Magn. Reson. Med*., 2010, **63**, 625–632.

(5) (*a*) D. F. Evans, *J. Chem. Soc*., 1959, **0**, 2003–2005; (*b*) E. M. Schubert, *J. Chem. Educ*., 1992, **69**, 62.

(6) G. A. Bain and J. F. Berry, *J. Chem. Educ*., 2008, **85**, 532–536.

(7) D. T. Sawyer, A. Sobkowiak and J. L. Roberts Jr., *Electrochemistry for Chemists*, 2nd edn, John Wiley & Sons, Hoboken, NJ, 1995.